

This Page Is Inserted by IFW Operations  
and is not a part of the Official Record

## **BEST AVAILABLE IMAGES**

Defective images within this document are accurate representations of the original documents submitted by the applicant.

Defects in the images may include (but are not limited to):

- BLACK BORDERS
- TEXT CUT OFF AT TOP, BOTTOM OR SIDES
- FADED TEXT
- ILLEGIBLE TEXT
- SKEWED/SLANTED IMAGES
- COLORED PHOTOS
- BLACK OR VERY BLACK AND WHITE DARK PHOTOS
- GRAY SCALE DOCUMENTS

**IMAGES ARE BEST AVAILABLE COPY.**

**As rescanning documents *will not* correct images,  
please do not report the images to the  
Image Problem Mailbox.**

16. (Twice Amended) The method of claim 9 7, wherein the polypeptide is modified with ~~one~~ two or more lipophilic moieties.
51. (Twice Amended) The method of claim 9 7, wherein the polypeptide is a fusion protein.
52. (Amended) The method of claim 9 7, wherein the *hedgehog* amino acid sequence is at least 95 percent identical to at least one of SEQ ID NO: 10, SEQ ID NO: 13, SEQ ID NO: 14, or SEQ ID No: 15, or an N-terminal fragment thereof of at least 50 contiguous amino acid residues ~~SEQ ID Nos. 10-18 or any fragment thereof that binds to a *patched* polypeptide.~~
53. (Amended) The method of claim 9 7, wherein the *hedgehog* amino acid sequence is identical to at least one of SEQ ID NO: 10, SEQ ID NO: 13, SEQ ID NO: 14, or SEQ ID No: 15, or an N-terminal fragment thereof of at least 50 contiguous amino acid residues ~~SEQ ID Nos. 10-18 or any fragment thereof that binds to a *patched* polypeptide.~~
55. (Amended) The method of claim 9 54, wherein the N-terminal fragments have a molecular weight of about 19 kD.

#### **REMARKS**

Claims 1-58 are the pending claims in the present application. Claims 1-11, 13-23, 30, 31, 41, 44-48, 50, and 51 were elected with traverse. Applicants will cancel non-elected claims upon indication of allowable subject matter. Please cancel, without prejudice, claims 7, 54, 56, 57 and 58. Applicants add new claims 59-73. Support for the subject matter of these claims is found throughout the specification. No new matter has been entered. Applicants respectfully request reconsideration in view of the following remarks. Issues raised by the Examiner will be addressed below in the order they appear in the prior Office Action. Applicants thank the Examiner and his Supervisor for courtesies extended during an interview at the United States Patent Office on October 7, 2002.

1-3. Applicants note with appreciation that the amendments put forth in Paper 19 have been entered in full. Claims 1-7 and 9-58 are pending.

4. Applicants note with appreciation that the objections to the specification are withdrawn in view of Applicants' amendments.

5-6. Applicants note that the rejections under 35 U.S.C. 101 and 35 U.S.C. 112, second paragraph, of claim 1-11, 13-23, 30, 31, 41, 44, 45-47, 48, 50 and 51 are withdrawn in view of Applicants' amendments.

7. Claims 1-7, 9-11, 13-23, 30, 31, 41, 44, 45-47, 48 and 50-58 are rejected under 35 U.S.C. 112, first paragraph, as allegedly containing subject matter that was not described in the specification in such a way as to enable one of skill in the art to practice the claimed invention. Applicants traverse this rejection to the extent that it is maintained in light of the amended claims.

The basis of the rejection appears to have three components. Firstly, the Examiner alleges that although Applicants have demonstrated that administration of a hedgehog polypeptide is efficacious in the protection and treatment of cisplatin-induced neuropathy, Applicants have allegedly failed to reasonably enable for methods of treating other neuropathies. Secondly, the Examiner alleges that although Applicants have demonstrated that Sonic hedgehog is useful in the methods of the present invention, Applicants have allegedly failed to reasonably provide methods which employ other hedgehog polypeptides. Finally, the Examiner alleges that although Applicants have demonstrated the efficacy of Sonic hedgehog in the methods of the present invention, Applicants have not reasonably enabled for methods of treating peripheral neuropathies using non-polypeptide agonists.

Applicants contend that the application, as filed, clearly contemplates that hedgehog agonists can be used in the treatment of a range of peripheral neuropathies including diabetic neuropathy (page 8, line 2 – page 9, line 2), and Applicants provide a working example demonstrating that Sonic hedgehog is efficacious in the treatment of cisplatin-induced neuropathy (Example 1). Additionally, Applicants note that significant evidence obtained since the filing of the present application indicates that, as contemplated in the specification, hedgehog polypeptides reduce the symptoms of other forms of neuropathy.

"Focus on ALS" is an article summarizing work presented at the Fifth Annual Diabetic Neuropathy Meeting which included a study demonstrating an improvement in both sensory and motor nerve function in diabetic mice treated for five weeks with Sonic hedgehog protein

("Focus on ALS", 2000, enclosed herewith as Exhibit 1). Additionally, Applicants submit herewith the declaration under 35 U.S.C. §1.132 of Karen Allendoerfer. This declaration summarizes a series of experiments which demonstrate that the reduction of Desert hedgehog expression in peripheral nerves of adult diabetic rats correlates with the onset of symptoms of diabetic neuropathy (Exhibit A). Furthermore, the declaration of Karen Allendoerfer summarizes experiments which demonstrate that administration of Sonic hedgehog improves both sensory and motor nerve conduction velocities in streptozotocin (STZ) treated diabetic rats.

Exhibit A shows the results of in situ hybridization analysis of the peripheral nerves of normal adult rats and STZ treated diabetic rats. Diabetes was induced in adult male rats with an intraperitoneal injection of streptozotocin (STZ). In situ hybridization analysis demonstrates that Dhh is expressed in the peripheral nerves of wildtype adult rats, but that this expression was severely reduced in the peripheral nerves of diabetic rats.

Exhibits B and C demonstrate that administration of Shh improved both motor nerve conduction velocity and sensory nerve conduction velocity in diabetic rats. Briefly, diabetes was induced in adult male rats with an intraperitoneal injection of STZ. Following 5 weeks of diabetes, rats were treated 3 times per week with either Shh or with a vehicle control, and these treatments were continued for 5 weeks. Shh was injected subcutaneously to the scruff of the neck, and administered at a dose of either 0.3, 1.0 or 3.0 mg/kg.

Diabetes impeded the progressive increase of both motor nerve conduction velocity and sensory nerve conduction velocity such that over the 10 week course of the study, diabetic rats have significantly lower MNCVs and SNCVs than non-diabetic rats. Exhibits B and C demonstrate that administration of Shh, but not vehicle, ameliorates these deficits and restores MNCV and SNCV to levels observed in non-diabetic rats. In Exhibit B, filled squares represent vehicle treated control animals, open squares represent Shh treated control animals, filled circles represent vehicle treated diabetic animals, and open circles represent diabetic animals treated with 1.0 mg/kg Shh.

The specification contemplates that hedgehog polypeptides can be administered to treat a variety of peripheral neuropathies. Furthermore, the specification is not purely prophetic and provides a working example which demonstrates that hedgehog polypeptides are efficacious in the treatment of cisplatin-induced neuropathy. The declaration of Karen Allendoerfer provides additional support to demonstrate that, as contemplated by the specification, administration of

hedgehog polypeptides treats a variety of peripheral neuropathies. Accordingly, Applicants contend that the claims are enabled throughout their scope.

In support of the second basis of the rejection, the Examiner has previously cited a few references in which a hedgehog polypeptide did not influence the fate of a particular neuronal cell type, and has pointed to the absence of data regarding the efficacy of non-Sonic hedgehog polypeptides in influencing adult cell types to argue that the effects of hedgehog polypeptides are extremely sensitive to the sequence of the hedgehog polypeptide. However, Applicants point out that substantial evidence exists to demonstrate that the hedgehog signaling pathway is not as sensitive to sequence variation in the hedgehog protein as the Examiner's comments suggest. Chang et al. demonstrated that mouse Sonic hedgehog can functionally substitute for either *Drosophila* hedgehog or quail Sonic hedgehog (Chang et al., 1994, enclosed herewith as Exhibit 2). Furthermore, much of the data found in the art demonstrating the efficacy of hedgehog polypeptides in influencing adult cell fates was obtained using a hedgehog polypeptide derived from a species other than the species in which the functional experiments were performed. For example, in the experiments summarized above in the declaration of Karen Allendoefer, human Sonic hedgehog was used in normal and diabetic rats. In experiments reported by Pola et al. which demonstrated a role for hedgehog polypeptides in promoting angiogenesis in adults, human Sonic hedgehog protein was used in mice (Pola et al. (2001), enclosed herewith as Exhibit 3). Applicants contend that the ability of hedgehog proteins derived from one species to function in another species demonstrates that hedgehog signaling is tolerant to some variation in the sequence of the hedgehog protein.

Applicants contend that the specification, especially in combination with the abundant evidence obtained since the filing of the present application, supports the enablement of the currently claimed invention. In accordance with MPEP 2164.05, when making a determination as to the enablement provided for the claimed invention, the evidence must be considered as a whole. Furthermore, "the evidence provided by the applicant need not be conclusive but merely convincing to one skilled in the art." (MPEP 2164.05). Applicants contend that this burden has been satisfied.

Furthermore, Applicants point out that even if the claims encompass certain inoperative embodiments, that does not undermine the enablement of the operative subject matter. In accordance with MPEP 2164.08(b), "[t]he presence of inoperative embodiments within the scope

of a claim does not necessarily render a claim nonenabled. The standard is whether a skilled person could determine which embodiments that were conceived, but not yet made, would be inoperative or operative with expenditure of no more effort than is normally required in the art.” This standard has been upheld in the courts, and permits a claim to encompass a finite number of inoperable embodiments so long as inoperable embodiments can be determined using methodology specified in the application without undue experimentation. See, for instance, *In re Angstadt*, 190 U.S.P.Q. 214 (CCPA 1976).

Finally, the Examiner contends that Applicants have failed to enable for other hedgehog agonist such as small molecule agonists. Applicants reiterate the arguments of record, and contend that the specification clearly contemplates the use of other non-hedgehog polypeptide agonists of hedgehog signal transduction in the presently claimed methods.

The specification provides a detailed discussion of hedgehog signaling, and clearly contemplates that a number of polypeptide and/or small molecule agonists can be used to agonize hedgehog signaling (page 47, lines 23-34). Additionally, the specification provides exemplary polypeptide (e.g., hedgehog polypeptides) and small molecule (e.g., PKA inhibitors) agonists which provide further guidance to one of skill in the art. Finally, the specification provides a detailed discussion of methods for screening for polypeptide and/or small molecule agonists of hedgehog signaling (page 48, line 6-page 50, line 30).

Given that the specification clearly contemplates a wide range of polypeptide and small molecule agonists of hedgehog signaling, provides exemplary hedgehog agonists, and provides methods that would allow one of skill in the art to identify other hedgehog agonists, Applicants maintain that the claims are enabled throughout their scope. Nevertheless, to expedite prosecution of claims directed to commercially relevant subject matter, Applicants have amended the claims to more particularly point out the hedgehog agonists for use in the claimed methods. Applicants’ amendments are not in acquiescence of the rejection, and Applicants reserve the right to prosecute claims of similar or differing scope.

The specification clearly contemplates the presently claimed methods, and provides working examples which demonstrate the efficacy of hedgehog polypeptides in treating peripheral neuropathy. Additionally, Applicants provide the declaration of Karen Allendoefer to further demonstrate that, as contemplated by the specification as filed, hedgehog polypeptides are useful in treating a range of peripheral neuropathies including diabetic neuropathy.

Accordingly, Applicants contend that the claims are enabled throughout their scope, and reconsideration and withdrawal of the rejection are respectfully requested.

8. Claims 1-8, 10, 11, 13, 14, 16-23, 30, 31, 41, 44, 45-47, 48, and 50-58 are rejected under 35 U.S.C. 112, first paragraph, as allegedly containing subject matter that was not described in the specification in such a way as to convey that the inventors had possession of the claimed invention. Applicants traverse this rejection to the extent that it is maintained in light of the amended claims.

Applicants maintain the arguments of record and contend that the application, as filed, provides ample support for a wide range of hedgehog agonists. Such agonists include hedgehog polypeptides and small organic molecules. Accordingly, Applicants contend that claims directed to hedgehog agonists are well supported by the specification and satisfy all of the requirements under 35 U.S.C. 112, first paragraph.

Nevertheless, to expedite prosecution of claims directed to commercially relevant subject matter, Applicants have amended the claims to more particularly point out the hedgehog agonists for use in the subject methods. Applicants' amendments are not in acquiescence of the rejection, and Applicants reserve the right to prosecute claims of similar or differing scope. Reconsideration and withdrawal of this rejection are respectfully requested.

9-10. Claims 1-4, 6, 7, 9-11, 13-18, 21, 30, 31, 41, 44-48 and 50-58 are rejected under 35 U.S.C. 102(b) as allegedly being anticipated by Ingham et al. Applicants traverse this rejection to the extent that it is maintained in light of the amended claims.

Ingham et al. fail to satisfy the criteria for anticipating Applicants' invention. Both the MPEP and the Federal Circuit support Applicants' contention that in order to anticipate or render obvious the claimed invention, the cited art must teach all the limitations of the claimed subject matter (MPEP 2131). "A claim is anticipated only if each and every element as set forth in the claim is found, either expressly or inherently described, in a single prior art reference." *Verdegall Bros. v. Union Oil Company of California*, 814 F.2d 628, 631, 2 USPQ2d 1051, 1053 (Fed Cir. 1987). "The identical invention must be shown in as complete detail as is contained in the .... claim." *Richardson v. Suzuki Motor Co.*, 868 F.2d 1226, 1236, 9 USPQ3d 1913, 1920

(Fed. Cir. 1989). The Ingham et al. application fails to teach the particular combination of elements of the pending claims.

Nor is the claimed subject matter obvious in view of the teachings of Ingham et al. Applicants contend that a valid patent may issue for a nonobvious species related to a prior patented invention, even though the improvement falls within the claims of that prior patent. A prior genus which does not explicitly disclose a species does not anticipate a later claim to that species. This position is well supported by the holdings of the Federal Circuit. See, for example, *Corning Glass Works v. Sumitomo Electric U.S.A.*, 868 F.2d 1251, 1262, 9 USPQ2d 1962, 1970 (Fed. Cir. 1989).

Applicants contend that the relationship between the pending claims and the cited art is largely analogous to the factual situation in the above example. Applicants assert that the presently claimed invention is a species which is unobvious and patentable over the generic teachings of Ingham et al.

Applicants contend that Ingham et al. fail to teach or suggest all the limitations set forth in the claims. Although Ingham et al. is broadly enabling and provides compositions and methods using *hedgehog* polypeptides, Ingham et al. fail to teach the benefits of the particular combinations of agents and mode of administration set forth in the pending claims. That is, although Ingham et al. broadly teach methods using *hedgehog* polypeptides, Ingham et al. provide no motivation to specifically select the particular lipophilic modifications or the particular methods, as presently claimed. MPEP 2144.08 outlines the guidelines for determining that a reference renders an invention obvious and directs the Examiner to “determine whether one of ordinary skill in the relevant art would have been motivated to make the claimed invention as a whole, i.e., to select the claimed species or subgenus from the disclosed prior art genus.” Applicants contend that Ingham et al. fail to provide motivation to select the specific classes of lipophilic modified *hedgehog* polypeptides for the treatment of peripheral neuropathy. Furthermore, the Examiner has not provided any evidence or additional references that would have motivated one of skill in the art to arrive at Applicants’ invention.

Applicants maintain that Ingham et al. fail to satisfy the criteria necessary for anticipating or rendering obvious Applicants’ invention. Nevertheless, to expedite prosecution of claims



directed to commercially relevant subject matter, Applicants have amended the claims to more particularly point out the features of the lipophilic modified hedgehog polypeptides. Applicants' amendments are not in acquiescence of the rejection, and Applicants reserve the right to prosecute claims of similar or differing scope. Reconsideration and withdrawal of this rejection is requested.

11. Claims 1-4, 6, 7, 9-11, 13-18, 21, 30, 31, 41, 44-48 and 50-58 are rejected under 35 U.S.C. 103(a) as allegedly being unpatentable over Ingham et al. in view of Porter et al. Additionally claims 1-4, 6, 7, 9-11, 13-18, 21, 30, 31, 41, 44-48 and 50-58 are rejected under 35 U.S.C. 103(a) as allegedly being unpatentable over Ingham et al. in view of Pepinsky et al. Applicants traverse these rejections to the extent that they are maintained in light of the amended claims.

Applicants have discussed in detail above why Ingham et al. does not anticipate the claimed subject matter. Both Pepinsky et al. and Porter et al. teach lipophilic modifications of *hedgehog* polypeptides. However, neither reference overcomes the deficiencies of Ingham et al. with regard to the particular lipophilic modifications of *hedgehog* polypeptides. Therefore, neither Porter et al. nor Pepinsky et al. overcome the deficiencies of Ingham et al. Accordingly, reconsideration and withdrawal of the rejection is requested.

12. Claim 22 is rejected under 35 U.S.C. 103(a) as allegedly being unpatentable over WO95/18856, Ingham et al., in light of Jonassen et al. Applicants traverse this rejection to the extent that it is maintained over the amended claims.

Jonassen et al. fail to overcome the deficiencies of Ingham et al. Jonassen et al. fail to teach or suggest methods of administering modified hedgehog polypeptide in vivo. Furthermore, Jonassen et al. fail to provide guidance for selecting the particular lipophilic modifications (N-terminal and/or internal amino acid residues) recited in the pending claims. Reconsideration and withdrawal of this rejection are respectfully requested.

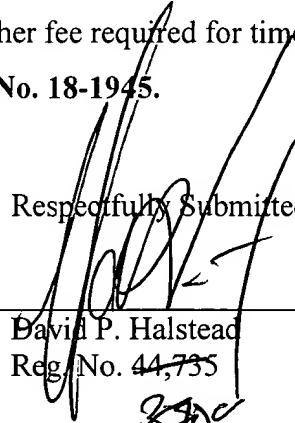
### CONCLUSION

In view of the foregoing amendments and remarks, Applicants submit that the pending claims are in condition for allowance. Early and favorable reconsideration is respectfully solicited. The Examiner may address any questions raised by this submission to the undersigned at 617-951-7000. Should an extension of time be required, Applicants hereby petition for same and request that the extension fee and any other fee required for timely consideration of this submission be charged to **Deposit Account No. 18-1945**.

Date: January 7, 2003

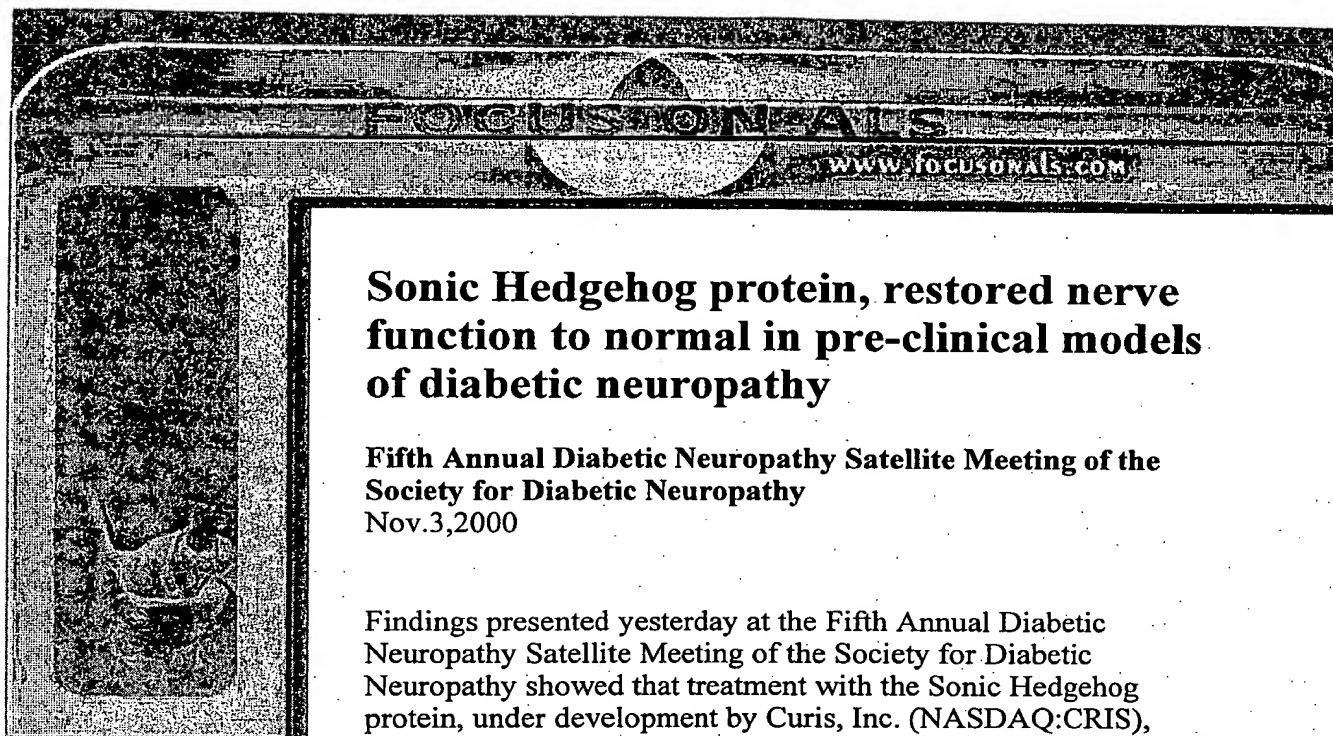
**Customer No: 28120**  
Docketing Specialist  
Ropes & Gray  
One International Place  
Boston, MA 02110

Respectfully Submitted,

  
\_\_\_\_\_  
David P. Halstead  
Reg. No. 44,735

28,700

28,700



## Sonic Hedgehog protein, restored nerve function to normal in pre-clinical models of diabetic neuropathy

**Fifth Annual Diabetic Neuropathy Satellite Meeting of the Society for Diabetic Neuropathy**  
Nov.3,2000

Findings presented yesterday at the Fifth Annual Diabetic Neuropathy Satellite Meeting of the Society for Diabetic Neuropathy showed that treatment with the Sonic Hedgehog protein, under development by Curis, Inc. (NASDAQ:CRIS), restored nerve function to normal in pre-clinical models of diabetic neuropathy.

Data from a study conducted by Dr. David Tomlinson of the University of Manchester showed complete restoration of both sensory and motor nerve function in pre-clinical models after that function was impaired. Five weeks after treatment on these models was begun, nerve conduction velocity measurements showed that sensory and motor function returned to pre-diabetic levels.

"These findings are an important part of the pre-IND program for a Hedgehog-based treatment for diabetic neuropathy at Curis," said Doros Platika, M.D., president and chief executive officer of Curis. "The repair and restoration of normal function in nerves that have been compromised by diabetes, as shown in this study, represents a key objective of the company's efforts in developmental biology, and we are moving forward aggressively to move such a therapy into human clinical testing.

"Of the estimated 15 million people with diabetes in the U.S., approximately six million patients have diabetic neuropathy. The market for treatments of this condition is estimated to be \$1.5 billion. Additional neurological diseases that may benefit from a Hedgehog-based therapy include multiple sclerosis, chemotherapy-induced neuropathy, Alzheimer's disease, and amyotrophic lateral sclerosis.

The family of Hedgehog proteins and their role in the development of neuronal cells and tissues are a key focus of ongoing research

Home  
What Is ALS?  
ALS Terms  
FAQ's  
ALS Facts  
Symptoms  
Diagnosis  
Treatments  
BiPAP/ CPAP  
Respiratory  
ALS Tips  
Research  
Resources  
Coping  
Caregiver  
Communication  
Nutrition  
Advocacy  
Links

Inspiration  
Quotes  
More Inspiration  
PALS pal  
Hospice  
Hope 4 Cure  
Memorial  
Morrie Schwartz  
My Story  
Lou Gehrig  
News  
Top Stories  
Stem Cell News

## EXHIBIT 1

E-Cards  
Profiles  
E-mail  
Thank you  
Disclaimer



We subscribe to the  
HON code principles  
of the  
Health On the Net  
Foundation



E-mail  
Your comments and  
suggestions are welcomed  
and appreciated.



"Rooster Romp"



I am a member of the  
HTML WRITERS GUILD

and development at Curis.

The development of innovative therapies by Curis to treat a variety of disorders, including diabetes, is focused upon recreating the conditions and redirecting key inducing molecules such as those involved in the Hedgehog pathway that control the normal growth and restore the function of tissues. Curis, Inc. is developing products based on technologies in the emerging field of regenerative medicine.

The Company is combining insights gained through the study of developmental biology with high-throughput screening capabilities, proteins, cells and biocompatible materials to facilitate the development of new regenerative medicine therapies. For more information, please visit the Curis web site.

- Air Force Base Eyed in ALS Cases
- Team finds "switch" to restore muscle
- Defective Gene Found For Amyotrophic Lateral Sclerosis With Dementia
- NIH Guidelines for research

[Back to Focus On ALS Home Page](#)  
[Back to Focus On ALS News Index](#)



[Back](#)

## Products, genetic linkage and limb patterning activity of a murine *hedgehog* gene

David T. Chang<sup>1</sup>, Alric López<sup>2</sup>, Doris P. von Kessler<sup>1</sup>, Chin Chiang<sup>1</sup>, B. Kay Simandl<sup>2</sup>, Renbin Zhao<sup>1</sup>, Michael F. Seldin<sup>3</sup>, John F. Fallon<sup>2</sup> and Philip A. Beachy<sup>1</sup>

<sup>1</sup>Howard Hughes Medical Institute, Department of Molecular Biology and Genetics, The Johns Hopkins School of Medicine, Baltimore, Maryland 21205, USA

<sup>2</sup>Department of Anatomy, Neuroscience Training Program, University of Wisconsin, Madison, Wisconsin 53706, USA

<sup>3</sup>Departments of Medicine and Microbiology, Duke University Medical Center, Durham, North Carolina 27710, USA

### SUMMARY

The *hedgehog* (*hh*) segmentation gene of *Drosophila melanogaster* encodes a secreted signaling protein that functions in the patterning of larval and adult structures. Using low stringency hybridization and degenerate PCR primers, we have isolated complete or partial *hh*-like sequences from a range of invertebrate species including other insects, leech and sea urchin. We have also isolated three mouse and two human DNA fragments encoding distinct *hh*-like sequences. Our studies have focused upon *Hhg-1*, a mouse gene encoding a protein with 46% amino acid identity to *hh*. The *Hhg-1* gene, which corresponds to the previously described *vhh-1* or *sonic* class, is expressed in the notochord, ventral neural tube, lung bud, hindgut and posterior margin of the limb bud in developing mouse embryos. By segregation analysis the *Hhg-1* gene has been localized to a region in proximal chromosome 5, where two mutations affecting mouse limb development previously

have been mapped. In *Drosophila* embryos, ubiquitous expression of the *Hhg-1* gene yields effects upon gene expression and cuticle pattern similar to those observed for the *Drosophila hh* gene. We also find that cultured quail cells transfected with a *Hhg-1* expression construct can induce digit duplications when grafted to anterior or mid-distal but not posterior borders within the developing chick limb; more proximal limb element duplications are induced exclusively by mid-distal grafts. Both in transgenic *Drosophila* embryos and in transfected quail cells, the *Hhg-1* protein product is cleaved to yield two stable fragments from a single larger precursor. The significance of *Hhg-1* genetic linkage, patterning activity and proteolytic processing in *Drosophila* and chick embryos is discussed.

Key words: mouse, *hedgehog*, genetic linkage, limb development, gene expression, *Hammertoe*, *Hemimelic extra toes*

### INTRODUCTION

Experimental manipulations of vertebrate embryos have revealed the existence of organizing centers that appear to function in the patterning of adjacent structures. The dorsal blastopore lip in *Xenopus*, for example, appears to control development of the major body axis (Spemann, 1933), while the posterior margin of the limb bud or ZPA (zone of polarizing activity or polarizing region) is capable of imposing pattern upon developing limbs (Saunders and Gasseling, 1968; Wolpert, 1969). Because these and other organizing centers contribute few of the cells that constitute the actual structure being formed, patterning activity is inferred to occur through the agency of molecules secreted from the organizing center. Until recently, however, little was known about the nature and identity of these molecules.

*Drosophila* development has long served as a model system for the study of molecules important in vertebrate developmental processes, including secreted signaling proteins. For example, the product of the *dpp* (*decapentaplegic*) gene, a member of the TGF- $\beta$  super-family of signaling molecules

which is expressed at the dorsal pole of the embryo, acts as a concentration-dependent factor capable of imposing pattern along the entire dorsal-ventral axis of the embryo (Ferguson and Anderson, 1992). The *wingless* (*wg*) segment polarity gene, a member of the *Wnt* super-family that also includes many vertebrate representatives (reviewed by Nusse and Varmus, 1992), encodes another signaling protein that acts at somewhat shorter range in segmentation and in patterning of the embryonic cuticle. Early expression of the *wg* gene in a stripe of cells bordering the parasegment boundary is required for maintenance of appropriate gene expression in an adjacent stripe of cells on the opposite side of the parasegment boundary (DiNardo et al., 1988; Martinez Arias et al., 1988); at a later stage, specification of appropriate differentiated fates depends upon expression of the *wg* product in neighboring cells (Baker, 1988; Bejsovec and Martinez-Arias, 1991; Dougan and DiNardo, 1992).

Another *Drosophila* segment polarity gene that has been implicated as encoding a signaling molecule with an important role in patterning is *hedgehog* (*hh*). Clones of mutant cells lacking *hh* function appear to affect adjacent structures in the

eye and cuticle of the *Drosophila* adult (Mohler, 1988; Heberlein et al., 1993; Ma et al., 1993). In the embryo, *hh* transcription is restricted to cells in a narrow stripe adjacent to and non-overlapping with the *wingless* stripe; *hh* mutations, however, affect gene expression and cuticle pattern elements in cells outside this zone of transcription (Mohler and Vani, 1992; Lee et al., 1992; Tabata et al., 1992; Tashiro et al., 1993). The notion that *hedgehog* encodes a secreted signaling molecule is also supported by other types of evidence – in vitro translated protein products can be secreted into microsomes (Lee et al., 1992) and immunostaining of *Drosophila* embryos shows that the *hh* protein is distributed in stripes that are broader than the stripes of *hh* transcription (Taylor et al., 1993; Tabata and Kornberg, 1994; von Kessler, D.V. and Beachy, P.A. unpublished observations). Molecular characterization of the *Drosophila hh* gene (Lee et al., 1992; Mohler and Vani, 1992; Tabata et al., 1992; Tashiro et al., 1993) revealed no sequence similarities to the products of other genes, despite the fact that many segment polarity genes do have homologues in other species (see Peifer and Bejsovec, 1992 for a review). More recently, however, several groups have demonstrated the existence of *hedgehog* homologs in chick, mouse, zebrafish and rat (Echelard et al., 1993; Krauss et al., 1993; Riddle et al., 1993; Roelink et al., 1994; S. C. Ekker and P. A. B., unpublished data).

Here we present evidence for broad evolutionary conservation of *hedgehog* sequences among invertebrate species. We also confirm the existence of a family of at least three mouse *hedgehog* homologues (Echelard et al., 1993) and demonstrate the existence of two new human *hedgehog* homologues. We show that *Hhg-1*, the mouse homologue which corresponds to the independently identified *vhh-1* and sonic *hedgehog* genes in the rat and the mouse (Roelink et al., 1994; Echelard et al., 1993), is expressed in the notochord, ventral neural tube, lung bud, hindgut and posterior limb bud margin in developing mouse embryos. To elucidate *Hhg-1* function, we first demonstrated that *Hhg-1* yields effects upon gene expression and cuticle pattern similar to those of the *Drosophila hh* gene when ubiquitously expressed in *Drosophila* embryos. We also found that grafts of cells expressing *Hhg-1* can impose pattern upon the developing chick limb. In both of these systems, the *Hhg-1* protein product is cleaved to yield two stable fragments from a single larger precursor. Consistent with a role in limb patterning, we mapped *Hhg-1* by segregation analysis to a region of mouse chromosome five with tight linkage to two previously mapped limb mutants. Proteolytic processing of *Hhg-1* products and their ability to function in *Drosophila* embryos as well as in vertebrate limb patterning suggests widespread conservation of the fundamental mechanisms underlying function of the *hedgehog* multi-gene family.

## MATERIALS AND METHODS

### Isolation of *hedgehog* homologues

Genomic clones from *Drosophila hydei* and the mosquito *Anopheles gambiae* were isolated by low-stringency screening (hybridization at 52°C, 6× SSC; washes in 2× SSC) of a *D. hydei* genomic library in the EMBL4 lambda phage vector (a gift of M. Claudia and D. Sullivan) and of an *A. gambiae* genomic library in the lambda phage vector DASH 2 (kindly provided by J. Kassis). The initial probe for this screen corresponded to positions 389–1801 (numbering according

to Lee et al., 1992), and further analysis of the *D. hydei* clone using exon-specific probes identified three hybridizing regions that corresponded to exons 1, 2 and 3 of *D. melanogaster hh*. The flour beetle (*Tribolium castaneum*; DNA a gift from Sue Brown), the leech (*Hirudo medicinalis*; DNA a gift from G. Aisemberg), the sea urchin (*Strongylocentrotus purpuratus*; DNA a gift from A. Cameron) and the mouse and human *hh*-like sequences were initially isolated by polymerase chain reaction (PCR) using primers degenerate for all possible coding combinations of the sequences underlined in Fig. 1. PCR amplifications contained from 100 ng to 2 µg genomic DNA (depending upon the genome size of the species), 2 µM of each primer, 200 µM dNTPs (Pharmacia), 1× reaction buffer (Boehringer-Mannheim) and 2.5 units Taq polymerase (Boehringer-Mannheim) in 50 µl reactions. Amplification was as follows: 94°C 5 minutes, addition of Taq polymerase at 75°C, followed by 94°C 1 minute, 52°C 1.5 minutes and 72°C 1 minute for 30 cycles and a final extension of 72°C for 5 minutes. All PCR products were cloned into pBluescript (Stratagene) prior to sequence determination. No *hh*-like sequences were obtained using DNA from *Dictyostelium* or from *C. elegans* using this approach.

Mouse clones obtained in this manner contained 144 bases of sequence between the primer ends and were labelled with [ $\alpha$ -<sup>32</sup>P]dATP and used for high stringency screens of mouse cDNA libraries made from whole 8.5 dpc embryonic RNA (Lee, 1990) and from 14.5 dpc embryonic brain in the  $\lambda$ ZAP vector (a gift from A. Lanahan). Several clones corresponding to *Hhg-1* were isolated and the largest, 2629 bp in length (pDTC8.0), was chosen for sequence analysis using dideoxy chain termination (Sanger et al., 1977) and Sequenase v2.0 (US Biochemicals). Compressions were resolved by using 7-deaza guanosine (US Biochemicals). Sequence analysis made use of the Geneworks 2.0 (IntelliGenetics) and MacVector 3.5 (IBI) software packages.

### Analysis of RNA expression in mouse and *Drosophila* embryos

For northern blot analysis, RNA from mouse embryos and from mouse adult tissues was isolated, electrophoresed in 1.2% agarose, blotted and probed, essentially as described by Ausubel et al. (1993). The probe used was made by random hexamer primed synthesis using the pDTC8.0 insert as a template in the presence of [ $\alpha$ -<sup>32</sup>P]dATP. Hybridizations and washes were performed under standard high stringency conditions (Ausubel et al., 1993).

In situ hybridization to sections of mouse embryos was essentially as described Wilkinson (1992), except that [ $\alpha$ -<sup>32</sup>P]rUTP was substituted in place of [ $\alpha$ -<sup>35</sup>S]rUTP for riboprobe synthesis. Briefly, 7.5–10.5 dpc mouse embryos were harvested, fixed in ice-cold 4% paraformaldehyde in PBS, dehydrated through an ethanol series, cleared in xylene and embedded in paraffin. 6 µm sections were floated on a 48°C water bath, transferred to AAS (3-aminopropyltriethoxysilane, Sigma) subbed slides, dewaxed with xylene and hybridized overnight to riboprobe in the sense or antisense orientations. Slides were washed under high-stringency conditions, dipped in Kodak NTB-2 emulsion and developed after a 10 day exposure. All sections were then stained for 30 seconds with haematoxylin (Polysciences) and mounted with Permount (Fisher). Sense and antisense probes were synthesized using a riboprobe synthesis kit from Stratagene with a 249 bp *Bam*HI/*Sma*I fragment of pDTC8.0 that extends from residues 297 to 380 within the *Hhg-1* open reading frame (Fig. 1) subcloned into Bluescript as template (pDTC1.8). Adobe Photoshop was used for superimposition of bright-field and dark-field views, collected in digital form using a Sony 3 CCD camera attached to a Zeiss Axioplan microscope and transferred directly to a Macintosh Quadra 800 equipped with a NuVista Video Capture Board. In situ hybridization to *Drosophila* embryos was performed according to standard methods (Tautz and Pfeifle, 1989). The *wingless* (*wg*) probe was made by random hexamer primed synthesis (Feinberg and Vogelstein, 1983) using a 2.2 kb *Hind*III/*Xba*I fragment from a

wg cDNA (gift from R. Nusse; Rijsewijk et al., 1987) as template. Probe synthesis was carried out in the presence of digoxigenin-dUTP (Boehringer Mannheim).

#### **Drosophila germ-line transformation and phenotypic analysis**

The *hshh* construct was made by inserting a blunted 1581 bp *MseI* fragment containing the full *hh* ORF (from 327 to 1908, Lee et al., 1992) into the *StuI* site of pCaSpeR-hs (Thummel et al., 1988; from C. Thummel, University of Utah, Salt Lake City). The *hsHhg-1* construct was made by inserting a blunted 1330 bp *Bsu36I/Eco57I* fragment from pDTC8.0 that contained the entire *Hhg-1* open reading frame into the *StuI* site of pCaSpeR-hs. *hshh* and *hsHhg-1* each were coinjected with *px25.2* into *w<sup>1118</sup>* embryos using a standard protocol for P element-mediated transformation (Rubin and Spradling, 1982). Germ line transformants with P element integration on the third chromosome were isolated for each construct; *hshh* was maintained as a homozygous stock and *hsHhg-1* was maintained over the TM3 balancer chromosome.

Embryos for cuticle analysis were collected and aged at 25°C and heat shocked for 1 hour at 37°C. After further incubation for 24 hours at 25°C, embryos were dechorionated, transferred to Hoyer's mountant (Wieschaus and Nusslein-Volhard, 1986) and incubated at 65°C for 5 hours. For in situ hybridization, *Drosophila* embryos from the *hs-hh*, *hs-Hhg-1* and *w<sup>1118</sup>* parent lines were collected for 5 hours at 25°C, aged an additional 5 hours at 25°C, heat shocked for 1 hour at 37°C and allowed to recover at 25°C for an additional hour before fixation.

#### **Chick limb patterning assays**

Isolation and characterization of the quail cell line QT6 has been described (Moscovici et al., 1977). QT6 cells were cultured on 3.5 cm uncoated plastic culture dishes (Falcon) in growth medium (M199 medium plus Earle's balanced salt solution [Gibco, Grand Island, NY] supplemented with 10% tryptose phosphate broth, 5% fetal calf serum, 1% dimethylsulfoxide, 100 U/ml of penicillin and 100 µg/ml of streptomycin) in a 5% CO<sub>2</sub> atmosphere.

QT6 cells were transiently transfected by a modified calcium phosphate method (Chen and Okayama, 1987). In brief, after preincubation in transfection medium (DMEM plus 5% fetal calf serum + 1% DMSO) 20–25 µg of precipitated DNA was added to 70–80% confluent QT6 cells in dishes. After overnight incubation, the DNA precipitate was removed and complete growth medium added. The pCIS plasmid, which carries a cytomegalovirus (CMV) promoter and SV40 intron and polyadenylation signal (Gorman, 1985), was used as the expression vector. Expression constructs included pCIS*lacZ* and pCIS*Hhg-1*, which contain *lacZ* and *Hhg-1* respectively under control of the CMV promoter. To assess transfection efficiency parallel plates were transfected with equimolar amounts of either pCIS-*lacZ* or pCIS*Hhg-1*.

For  $\beta$ -galactosidase activity staining, cells and limb buds were fixed 5 minutes and 1 hour, respectively, in PBS containing 2% formaldehyde and 0.2% glutaraldehyde. After rinsing in PBS, samples were incubated in X-gal cocktail (1 mg/ml X-gal (5-bromo-4-chloro-3-indolyl 5-b-D-galactopyranoside), 2 mM MgCl<sub>2</sub>, 16 mM K<sub>3</sub>Fe(CN)<sub>6</sub>, 16 mM K<sub>4</sub>Fe(CN)<sub>6</sub>) for 18–24 hours at 22°C.

Transiently transfected QT6 cells were scraped from tissue culture plates with a Teflon scraper (Falcon) and dissociated by repeated pipetting. Poly-D-lysine (Sigma, P1149) was added to the cell suspension to a concentration of 33 µg/ml. Cells were then pelleted by centrifugation at 1 × 10<sup>3</sup> revs/minute on a benchtop microfuge for 10 seconds. Wedge-shaped fragments were excised from the pelleted cells and grafted to anterior, mid-distal, or posterior slits made with fine forceps in stage 20–21 chick wing buds (Riley et al., 1993). Embryos harvested at day 10 were fixed overnight in 10% formaldehyde, stained with Victoria blue and cleared in methyl salicylate (see Riley et al., 1993).

#### **Detection of *Hhg-1* protein**

Region-specific antibodies were generated by immunization of New Zealand White rabbits with PCR-generated, His<sub>6</sub>-tagged fusions (in the vector pTrcHis from InVitrogen, San Diego, CA) to residues 25–159 (N-terminal) and 202–389 (C-terminal) of the *Hhg-1* ORF (Fig. 1). Following repeated boosts, reactive sera were purified using affinity matrices carrying fusions of glutathione-S-transferase to the same portions of the *Hhg-1* ORF (in the vector pGEX from Amrad, Melbourne, Australia). Specific antibodies were eluted with a buffer containing 100 mM glycine-HCl at pH 2.5 (Harlow and Lane, 1988).

For immunodetection, samples of transfected and untransfected QT6 cells and of heat-shocked wild-type and *hsHhg-1* *Drosophila* embryos were suspended and boiled in sample loading buffer and electrophoresed in 12% polyacrylamide-SDS gels (Laemmli, 1970). Following transfer to nitrocellulose (Burnette, 1981), proteins were detected by chemiluminescence (with the ECL kit from Amersham), with affinity purified anti-*Hhg-1* antibodies at a dilution of 1/300 and HRP-conjugated goat anti-rabbit 2° antibody (Jackson ImmunoResearch, Baltimore MD) at a dilution of 1/10,000.

#### **Chromosome localization of *Hhg-1***

C3H/HeJ-*gld* and *Mus spretus* (Spain) mice and [(C3H/HeJ-*gld* × *Mus spretus*)F<sub>1</sub> × C3H/HeJ-*gld*] interspecific backcross mice were bred and maintained as previously described (Seldin et al., 1988). *Mus spretus* was chosen as the second parent in this cross because of the relative ease of detection of informative restriction fragment length variants (RFLV) in comparison with crosses using conventional inbred laboratory strains.

DNA isolated from mouse organs by standard techniques was digested with restriction endonucleases and 10 µg samples were electrophoresed in 0.9% agarose gels. DNA was transferred to Nytran membranes (Schleicher & Schuell, Inc., Keene, NH), hybridized at 65°C and washed under stringent conditions, all as previously described (Sambrook et al., 1989). Clones used as probes in the current study included a ~500 bp 3'-UTR of *Hhg-1*, a quinoid dihydropteridine reductase (Qdpr) clone, DHPR13 (Lockyer et al., 1987) and an interleukin 6, (Il-6) specific clone, 27-4 (Mock et al., 1989).

Gene linkage was determined by segregation analysis (Green, 1981). Gene order was determined by analyzing all haplotypes and minimizing crossover frequency between all genes that were determined to be within a linkage group. This method resulted in determination of the most likely gene order (Bishop, 1985).

#### **Characterization of *Hhg-1* sequences in *Hm* and *Hx* mutants**

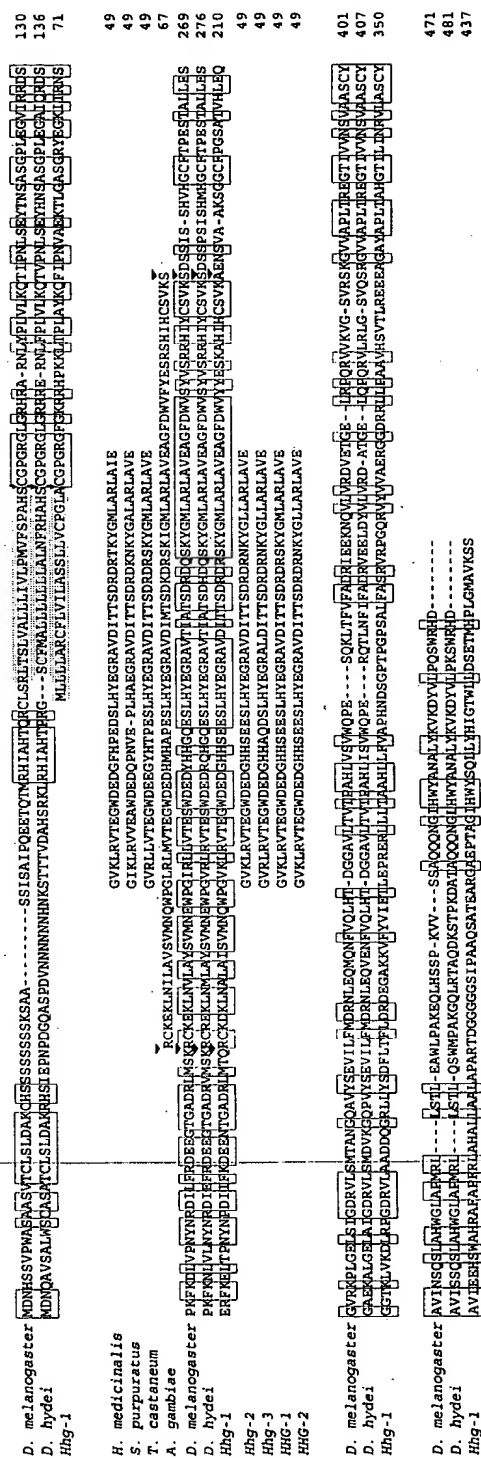
DNA from heterozygous *Hm* (AKR.C3H-*Ca Hm Sl*) and heterozygous *Hx* (B10.D2/nSn-*Hx*+) mutant individuals were obtained from Jackson Laboratory and digested with *EcoRI*, *BamHI*, *TaqI*, *HindIII*, *AluI*, *RsaI*, *DpnI*, *HinfI* and *HinPI*. These digests were electrophoresed, blotted and probed as above with <sup>32</sup>P-labelled pDTC8.0 and compared to similarly digested and probed DNAs from parental strains. No differences in restriction fragment lengths were detected for either mutant. This analysis would have detected differences as small as 100 bp.

*Hhg-1* coding sequences were isolated by PCR amplification from genomic DNA of individuals heterozygous for the *Hx* mutation (B10.D2/nSn-*Hx*+, Jackson Labs). Analysis included eleven independent clones representing coding sequences from exon one, fourteen independent clones representing coding sequences from exon two and eight independent clones representing coding sequences from exon three.

## **RESULTS**

### **Isolation of *hedgehog* homologues**

As a first step toward isolation of *hedgehog* homologues from distant species, we used low-stringency hybridization to isolate



genomic *hh* clones from two other dipterans, *Drosophila hydei* and the mosquito *Anopheles gambiae*. We then used the polymerase chain reaction (PCR) with degenerate primers from conserved regions within the second exon (underlined regions in Fig. 1) to isolate single *hh*-like sequences from genomic DNA of the flour beetle, leech and sea urchin, and multiple sequences from mouse and man. No *hh*-like sequences were obtained using DNA from *Dictyostelium* or from *C. elegans* by this approach. From sequence comparisons, human PCR fragments 1 and 2 appear to correspond most closely to mouse fragments 1 and 2, respectively.

Our focus here is primarily upon one of the three mouse clones, *Hhg-1*, which when used as a probe yielded a 2.0 kb clone from a 8.5 dpc mouse embryonic cDNA library and a 2.7 kb clone from a 14.5 dpc embryonic cDNA library. The 2.7 kb cDNA appears to represent a nearly full-length mRNA because it corresponds to a 2.8 kb band detected by hybridization on a northern blot (see below). The largest methionine-initiated open reading frame within this cDNA encompasses 437 codons and is preceded by one in frame upstream stop codon (not shown). Sequence comparisons indicate that the protein encoded by *Hhg-1* is identical to the independently characterized mouse *Shh* (Echelard et al., 1993) except for an arginine to lysine difference at residue 122. *Hhg-1* also corresponds closely to the rat *vhh-1* gene (97% amino acid identity; Roelink et al., 1994), the chicken *Sonic hedgehog* (81% identity; Riddle et al., 1993) and *Shh* from the zebrafish (68% identity; Krauss et al., 1993; Roelink et al., 1994; S.C. Ekker and P.A.B., unpublished data). The PCR-generated fragments *Hhg-2* and *Hhg-3* appear to correspond to the *Indian* and *Desert* classes of mouse *hedgehog* genes, respectively (Echelard et al., 1993).

Alignment of the *Hhg-1* open reading frame with the two *Drosophila hh* sequences (Fig. 1) shows that all three proteins contain hydrophobic amino acid sequences near their amino-termini; the hydrophobic stretches within the *D. melanogaster* protein (residues 64 to 83) and within the mouse protein are known to act efficiently as signal sequences for cleavage (Lee et al., 1992, and J. J. Lee and P. A. B., unpublished data). Both *Drosophila* signal sequences are unusual in their internal locations, while the hydrophobic stretch of the mouse gene occurs at the extreme amino-terminus, a more conventional location for cleaved signal sequences. Although portions of

Fig. 1. Multiple mammalian and invertebrate *hedgehog*-like sequences. The *Drosophila melanogaster hedgehog* open reading frame is shown aligned with a complete *hedgehog* coding sequence deduced from genomic sequence for *Drosophila hydei* and a complete mouse coding sequence (*Hhg-1*) deduced from a cDNA clone. Amino acid identities between these complete sequences are boxed, Kyte-Doolittle hydrophobic domains are shaded, predicted signal sequence cleavage sites (von Heijne, 1986) are indicated by an arrow; and intron/exon boundaries are marked by triangles. Below these complete sequences are shown partial sequences deduced from cloned PCR products for two other mouse genes (*Hhg-2* and *Hhg-3*) and two human sequences (*HHG-1* and *HHG-2*). Sequences from invertebrate species above the complete sequence alignments include partial sequences for the mosquito *Anopheles gambiae* (from a genomic clone) and PCR-derived sequences from the flour beetle, *Tribolium castaneum*, the urchin, *Strongylocentrotus purpuratus* and the leech, *Hirudo medicinalis*. Degenerate primers used for PCR reactions incorporated sequence from the underlined portion of the *D. melanogaster* sequence.



sequence N-terminal to the *Drosophila* signal sequences are conserved, suggesting a functional role, the mouse mouse gene lacks this region.

The overall level of amino acid identity between *Hhg-1* and *hh* carboxy-terminal to the signal sequences is 46%. A closer examination shows that the amino terminal portion, from residues 25 to 187, displays 69% identity, while remaining residues in the carboxy-terminal portion display a much lower 31% identity. Like *hh*, the *Hhg-1* coding sequence is divided into three exons and the boundaries of these exons are at the same positions within coding sequence as those of the three *Drosophila hh* exons (see Fig. 1). Curiously, the boundary between coding sequences of the second and third exons occurs near the transition from high to low levels of overall sequence conservation. The coincidence of these two boundaries suggests a possible demarcation of functional domains within these proteins. This location within *Hhg-1* coding sequence

also coincides approximately with the site of a presumed proteolytic cleavage (see below).

#### Expression of *Hhg-1* in mouse embryos

We began our analysis of *Hhg-1* expression by hybridization of a  $^{32}$ P-labelled *Hhg-1* probe to a northern blot of RNA isolated from embryos ranging from 8.5 to 18.5 dpc. A band of ~2.8 kb was detected at each stage, with a peak at day 10.5 (Fig. 2). These results are similar to those reported by Echelard et al. (1993) for *Shh* except that we detect the 2.8 kb RNA throughout embryogenesis. To obtain more detailed spatial and temporal information regarding *Hhg-1* expression, sections from 7.5, 8.5, 9.5 and 10.5 dpc embryos were hybridized to a  $^{33}$ P-labelled antisense RNA probe under stringent hybridization and wash conditions (see Materials and methods); the corresponding sense RNA probe was used as a control. Selected sections from these *in situ* hybridizations are presented in Figs 3-5 and described below.

In the 7.5 dpc embryo, *Hhg-1* expression is confined to anterior midline mesoderm. No expression is seen in the overlying ectoderm (Fig. 3B,C) or in other embryonic or extraembryonic tissue (data not shown). Transverse sections confirm restriction of expression in the early gastrula to axial mesoderm (Fig. 3D-F); this mesodermal expression extends caudally with retraction of the node and is maintained through to formation of the notochord by 8.5 dpc (data not shown).

At 9.5 dpc, well after neural tube formation, strong expression of *Hhg-1* is seen in the entire notochord and in the ventral midline of caudal portions of the neural tube. More rostrally within the neural tube, *Hhg-1* expression extends ventrolaterally to encompass ~40% of the ventral neural tube at its maximum extent in the midbrain. Even more rostrally in the midbrain, midline expression is lost but reappears in a portion of the diencephalon (Fig. 4B). Horizontal sections demonstrate that expression rostral to the midbrain (Fig. 4C) splits and extends bilaterally (Fig. 4D,E), finally re-uniting in the ventral

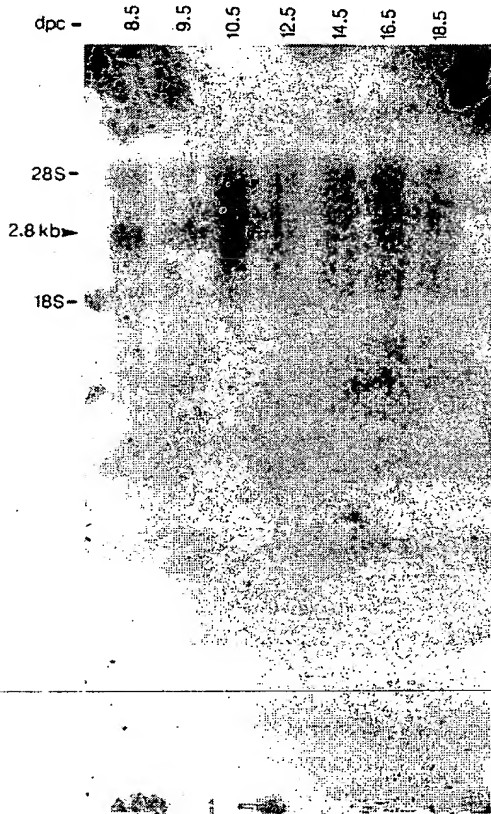


Fig. 2. Electrophoretic analysis of *Hhg-1* RNA. Each lane contains 10  $\mu$ g total RNA from mouse embryos staged as indicated above the lanes (dpc, days post coitum). The probe, made from the full length *Hhg-1* cDNA, detected a ~2.8 kb band (indicated by arrowhead) in RNA from all stages of embryos examined. The upper band comigrates with the 28S RNA and is due to non-specific hybridization.

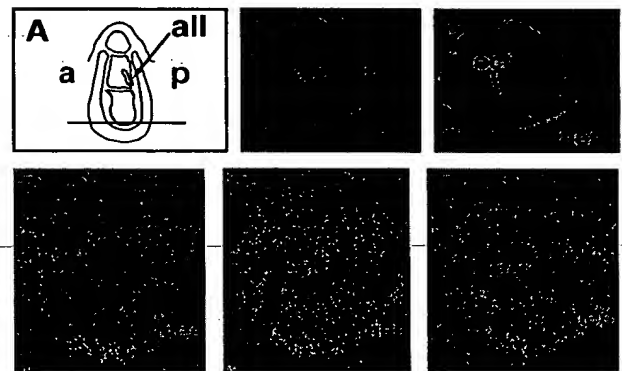


Fig. 3. *Hhg-1* expression at late gastrulation. (A) Schematic diagram showing 7.5 dpc mouse embryo, at late gastrulation. (B,C) Midsagittal sections through the egg cylinder showing hybridization in the axial mesoderm. (D-F) Adjacent horizontal sections through the egg cylinder at the level indicated in A. Note the hybridization in the midline mesoderm (asterisk). a, anterior; all, allantois; ect, ectoderm; mes, mesoderm; p, posterior.

midline of the diencephalon (Fig. 4B,E). *Hhg-1* expression thus is confined to a ring of cells in the ventral surface of the midbrain-diencephalic region. *Hhg-1* expression in the 10.5 dpc embryo is similar to that of the 9.5 dpc embryo, with strong expression in the notochord and most of the ventral neural tube and rostral neural tube expression remaining restricted to a ring of ventral cells. *Hhg-1* expression can also be observed in endoderm lining the future pharynx and foregut, with more intense expression occurring in the budding lungs; expression can also be detected in the hindgut. Finally, expression of *Hhg-1* in the limb buds at 10.5 dpc is restricted to the posterior margins of the forelimb (Fig. 5G-J) and hindlimb (data not shown). This expression clearly is restricted to the mesoderm and is absent from the overlying ectoderm, including the apical ridge. Our analysis of *Hhg-1* expression in the mouse embryo is consistent with that presented for *Shh* (Echelard et al., 1993) and for *vhh-1* in the rat embryo (Roelink et al., 1994).

#### *Hhg-1* can function in *Drosophila* embryos

As a first step toward understanding the function of mouse *hedgehog* genes, we compared the effects of *Hhg-1* and *Drosophila hh* when ectopically expressed in *Drosophila* embryos under control of a heat inducible promoter. As described in Materials and Methods, germ-line insertions were made by P-element-mediated transformation of each gene cloned downstream of the *Drosophila hsp70* promoter. Our analysis focused on one transformant line for each construct, designated *hshh* and *hsHhg-1*. Transcription of *hh* in the *Drosophila* embryo is normally restricted to a thin stripe of cells posterior to the parasegment boundary in each segment; expression of the *wingless* (*wg*) gene is normally restricted to a thin stripe of cells anterior and immediately adjacent to the *hh* stripe. Previous studies have demonstrated a dependence upon *hh* function for the maintenance of *wingless* expression (DiNardo et al., 1988; Martinez Arias et al., 1988); the spatial restriction of *wg* expression to this thin stripe is thought to result from limited diffusion of the signal encoded by *hh*. Ectopic expression of *hh* thus would be expected to cause an expansion in the domain of *wg* expression.

As shown in Fig. 6D,E, ubiquitous expression of *hh* induced by heat shock indeed causes an expansion in the extended germ band expression domain of the *wingless* gene, as has also been demonstrated by Ingham (1993). In

addition, ectopic expression of *hh* produces consistent alterations in the size and orientation of denticles in the ventral cuticle (Fig. 6F; see Bejsovec and Wieschaus, 1993, for a description of the wild-type denticle pattern). The simplest interpretation of these changes is that bristle rows 4, 5 and 6 are replaced by bristles of size, shape and polarity normally associated with the denticles in rows 2 and 3, and our observations are again consistent with those of Ingham (1993). Neither of these changes occur in heat shocked wild-type embryos (Fig. 6A,C).

Similar analyses of ectopically expressed *Hhg-1* also reveal an expansion in the *wg* expression domain and effects upon the denticles in rows 4, 5 and 6 (Fig. 6G,I). The early effect on *wg*

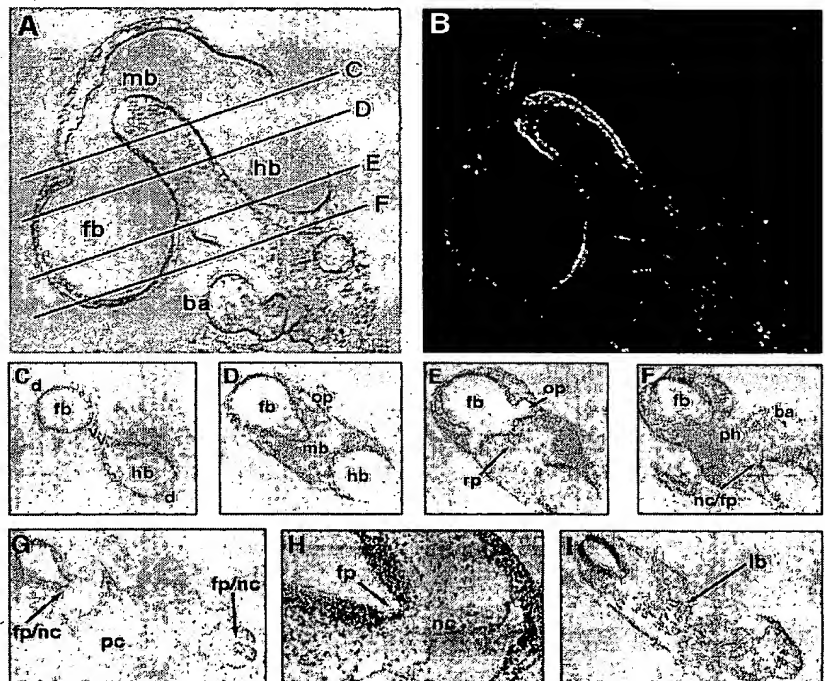
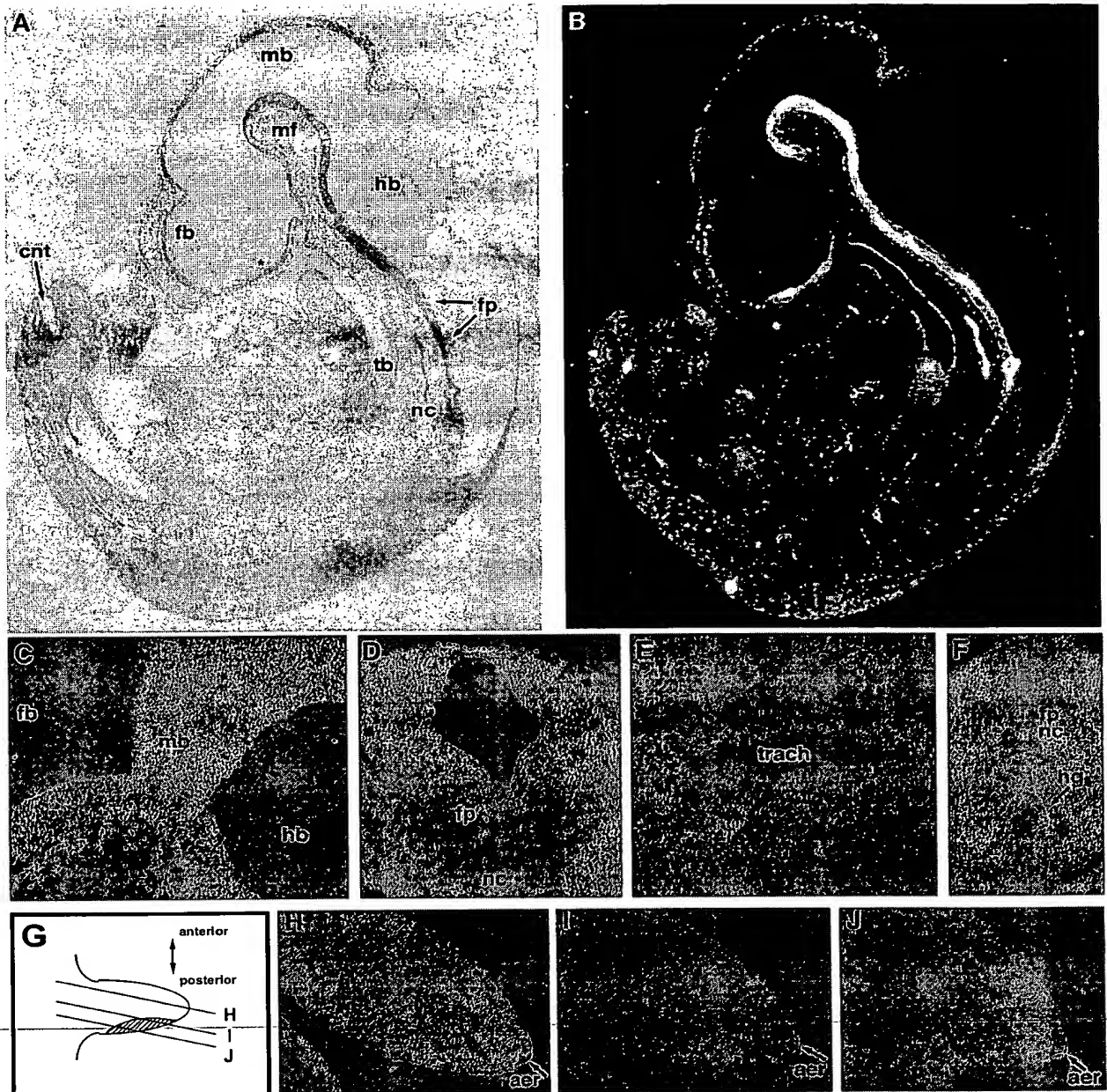


Fig. 4. *Hhg-1* expression in the 9.5 dpc embryo. (A,B) Bright and dark field views of a parasagittal section from a 9.5 dpc mouse embryo showing hybridization in the ventral midbrain and in a small patch of the ventral diencephalon. (C-F) Serial horizontal sections from superior to inferior levels in the head region of a 9.5 dpc mouse embryo. Broad, intense ventral hybridization is observed in the boundary region of the midbrain and forebrain (C). Rostrally, ventral-most expression is lost leaving two ventral/lateral domains of neural tube expression in cells adjacent to the optic vesicle. (D,E). Expression re-unites in a single midline domain of ventral neural tube cells overlying the pharyngeal lumen. Caudal to the hindbrain, neural tube expression is confined to the ventral midline (C-E) and expression is seen in the notochord beginning at its most rostral point (F). (G) Horizontal section at the level of the pericardiac region. The neural tube is cut twice in cross section at these levels and expression is likewise seen in floor plate and notochord of both cross sections. (H) Higher magnification view of G showing intense hybridization to floor plate and notochord. (I) Horizontal section at a lower level showing expression in the developing lung bud. In F, G and I, note the closer apposition of notochord to neural tube at more extreme rostral and caudal levels, indicative of an earlier stage of maturation relative to the intermediate level shown in H. ba, branchial arch; d, dorsal; fb, forebrain; fp, floor plate; lb, lung bud; mb, midbrain; nc, notochord; op, optic vesicle; pc, pericardiac region; ph, pharyngeal lumen; rp, Rathke's pouch; v, ventral.



**Fig. 5.** *Hhgl-1* expression in the 10.5 dpc embryo. (A,B) Bright- and dark-field views of a sagittal section from a 10.5 dpc mouse embryo showing intense hybridization in the ventral neural tube and notochord, ventral diencephalic region (asterisk), and tracheal branch point. (C) Horizontal section showing hybridization in the ventral epithelium of the midbrain. (D) Horizontal section at lower level showing expression in floor plate and notochord. (E) Horizontal section showing hybridization in the epithelia of the tracheal lumen. (F) Horizontal section showing continued expression in the floor plate and notochord at caudal levels and expression in the epithelia of the hindgut. (G) Schematic diagram of developing limb, and reconstruction of expression from serial sections. Lines indicate approximate levels of sections shown in H-J. (H-J) Anterior to posterior sections of developing forelimb. Intense expression is observed in the posterior but not anterior mesoderm. No expression is observed in the apical ectodermal ridge. aer, apical ectodermal ridge; cnt, caudal neural tube; fb, forebrain; fp, floor plate; hb, hindbrain; hg, hindgut; mb, midbrain; mf, mesencephalic flexure; nc, notochord; tb, tracheal branch point; trach, tracheal lumen.

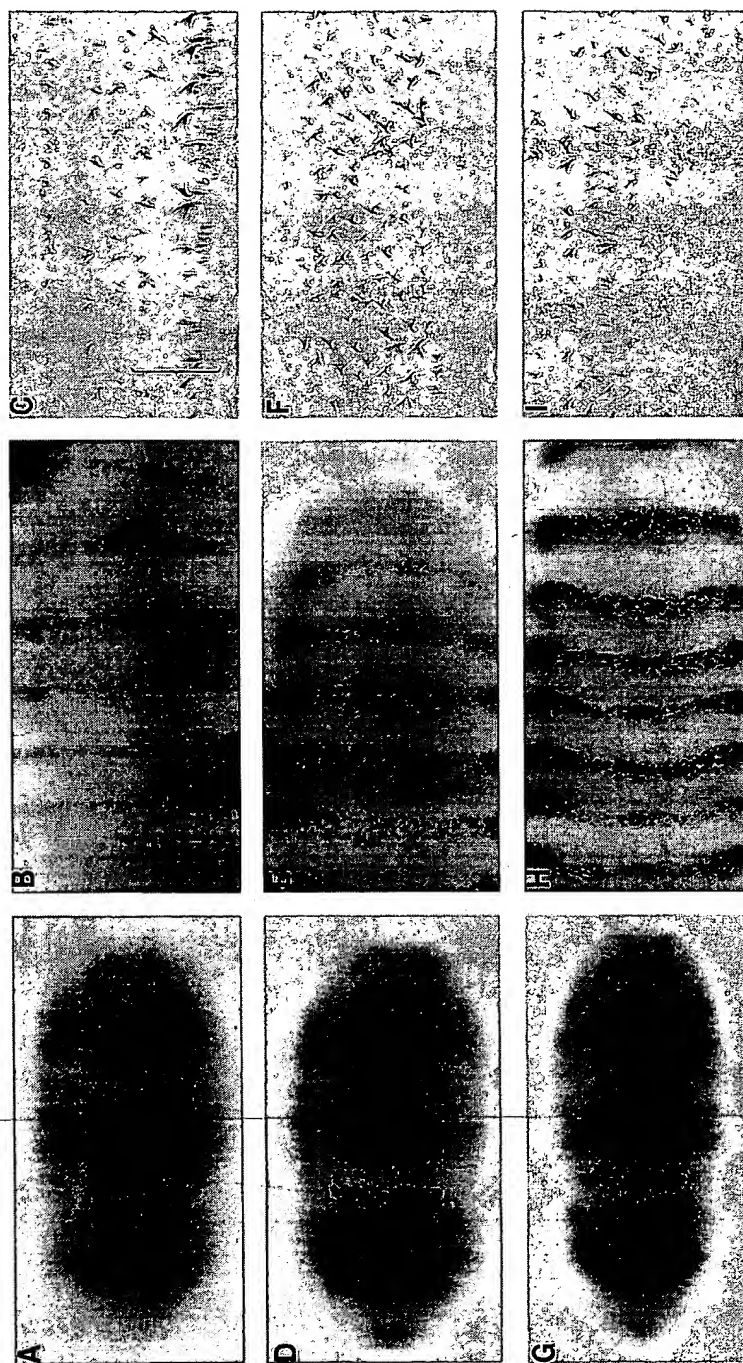


Fig. 6. Ectopic expression of *Hh* in the *Drosophila* embryo. A, B, D, E, G and H show ventral views of germ-band-extended (A, D, G) and retracted (B, E, H) embryos which have been heat shocked and processed for in situ hybridization to detect *wingless* RNA expression. C, F and I show the pattern of ventral denticles within a single segment from heat-shocked embryos just prior to hatching. The genotypes of embryos in A-C are *w<sup>1118</sup>*

(wild-type control), while embryos in D-F and G-I, respectively, carry the *hsh/h* and *hsh/Hg-1* construct (see text). Note that, relative to wild type (A, B), the *wingless* stripes are expanded at the extended and retracted germ band stages for embryos carrying the *hsh/h* (D, E) and *hsh/Hg-1* (G, H) constructs. Note also that the wild-type polarity and character of the bristle rows 4-6 (bracketed portion of C; see text) are altered in F and I.

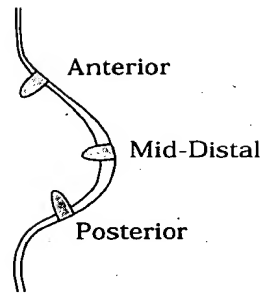


Fig. 7. Graft sites for limb patterning assays.

expression is indistinguishable from the *hh* effect. The denticles appearing in place of the posterior three denticle rows, however, appear more disorganized, with occasionally a missing denticle row and in some cases an unusual posterior row of anteriorly oriented denticles (Fig. 6I).

The patterns of *wg* expression thus far described pertain to the extended germ band stage. We also examined, however, the effects of ectopic *hh* and *Hhg-1* expression upon later stage embryos which had completed or nearly completed the process of germ band retraction. As shown in Fig. 6B,E,H, the *wg* expression domain is expanded relative to the wild type even at this later stage. The competence of cells in the expanded *wg* domain to respond to the ectopic *hh* signal at this late stage reveals a new requirement for temporal and spatial expression of candidate receptors for the *hh* signal (see Discussion).

#### Patterning activity of *Hhg-1* in the developing chick limb

*Hhg-1* expression in mouse limb buds is restricted to mesoderm along the posterior margin of the limb bud (Fig. 5G-I), a location reminiscent of the polarizing region in the chick limb bud. Given the ability of *Hhg-1* to function in as diverged a species as *Drosophila* (see above) and in light of previous reports of chick limb patterning activity present in grafts derived from mouse limb buds (Tickle et al., 1976; Fallon and Crosby, 1977), we tested the possibility that *Hhg-1* encodes an

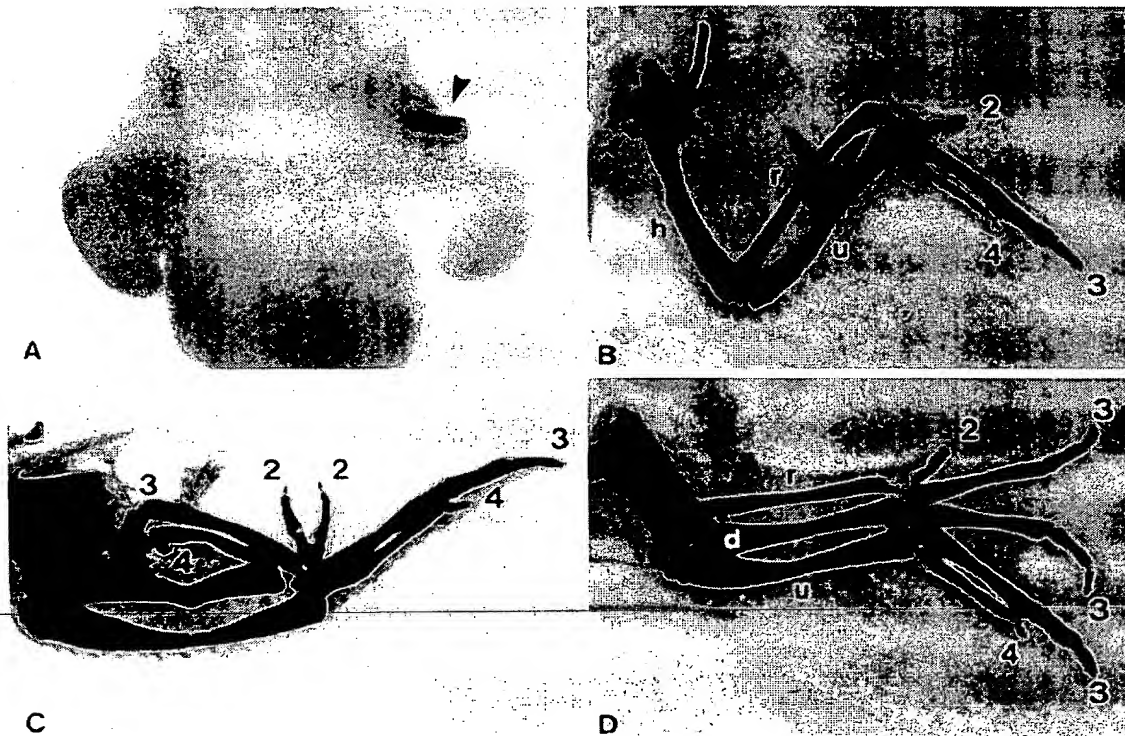


Fig. 8. Limb patterning activity of *Hhg-1*. Grafts of QT6 cells transfected with pCISlacZ (A) or pCISHhg-1 (B,C,D) were made to the anterior border (A,C) the posterior border (B) or to the mid-distal border (D) of forelimb buds within chick embryos at stage 20. The embryo in A was fixed 24 hours after grafting and stained for  $\beta$ -galactosidase activity (positive region indicated by arrowhead). Embryos in B-D were fixed, stained and cleared 7 days after grafting. The posterior border graft in B resulted in a normal limb skeleton (h, humerus; r, radius; u, ulna; 2, 3 and 4 indicate digit identities). The anterior border graft in C caused a mirror image duplication of the manus with a digit pattern of 4-3-2-2-3-4. The mid-distal border graft in D induced skeletal duplications of digits and of the forearm: d indicates a duplicated forearm bone that probably is an ulna; the digit pattern from anterior is 2-3-3 followed by the normal 3-4.



activity capable of imposing pattern upon chick limbs. The strategy for these experiments involved high-efficiency transient transfection of the QT6 quail cell line (Moscovici et al., 1977), followed by grafting of wedge-shaped sections of transfected cell pellets to anterior, mid-distal or posterior borders of stage 20-21 chick wing buds (see Fig. 7). Initial transfections using the bacterial  $\beta$ -galactosidase expression gene in the vector pCIS (Gorman, 1985), which carries a cytomegalovirus promoter and an SV40 intron and polyadenylation signal, yielded expression in greater than 90% of the QT6 cells plated for transfection.

Fig. 8 shows that grafts of cells transfected with a *Hhg-1*-expression construct to anterior and mid-distal but not posterior locations within developing limb buds induced duplications of digits. Duplications induced by anterior border grafts were in mirror-image orientation relative to the normal pattern, with a typical sequence of digits shown in Fig. 8C (4-3-2-2-3-4). Mid-distal grafts commonly yielded digits in the sequence 2-3-3-3-4, with divergent curvature of adjacent third digits indicative of the location of the graft site (Fig. 8D). Grafts of  $\beta$ -galactosidase-expressing cells or posterior grafts of *Hhg-1*-expressing cells, in contrast, did not alter normal limb pattern (Fig. 8A,B). With respect to digit duplications and polarity, all grafts of *Hhg-1* expressing cells act as posterior organizing centers, much in the same manner observed for polarizing region grafts (Saunders and Gasseling, 1968).

Curiously, we observed duplications of proximal skeletal elements such as the humerus, radius and ulna at a frequency of 65% in mid-distal border grafts (Fig. 8D; see Table 1), but never with anterior border grafts (Fig. 8C; see Table 1). To our knowledge, a strong correlation between graft location and duplication of proximal skeletal elements has not been previously noted, although previously reported results are consis-

tent with our observation (see Discussion). The overall level of proximal or distal element duplications in all limbs receiving anterior or mid-distal border grafts of *Hhg-1*-expressing cells was 86.5% (Table 1). These percentages are similar to those reported by Riddle et al. (1993) following anterior grafts of cells infected with a retrovirus carrying *Shh*, a *hedgehog* family member in the chicken that probably corresponds to *Hhg-1*.

#### Proteolytic processing of the *Hhg-1* protein product

We have used affinity purified antibodies directed against epitopes from two distinct portions of the *Hhg-1* ORF (Fig. 9A) to confirm that *Hhg-1* encoded protein indeed is expressed in both systems where we have assayed for *Hhg-1* activity. As shown in the immunoblots of Fig. 9B, QT6 cells transfected with the pCIS*Hhg-1* expression vector produce a polypeptide species of  $\sim 45 \times 10^3 M_r$  which is detected by both N- and C-terminal specific antibodies in transfected cells (lanes 1 and 3, respectively). In addition, a  $\sim 19 \times 10^3 M_r$  species is specifically detected by the N-terminal antibody while the C-terminal antibody specifically detects a  $\sim 28 \times 10^3 M_r$  species. Neither the

**Table 1. Skeletal element duplications induced by grafts of QT6 cells transfected with pCIS*Hhg-1***

Percentage of most posterior duplicated digit (n)				
Graft (n)	II	III	IV	Normal
Anterior hedgehog (29)	14% (4)	41% (12)	31% (9)	14% (4)
Mid-distal hedgehog (17)	17.5% (3)	65% (11)	0 (0)	17.5% (3)
$\beta$ -galactosidase (11)	0	0	0	100% (11)
Posterior hedgehog (7)	0	0	0	100% (7)

Percentage of proximal element duplications* (n)				
Graft (n)	Radius	Ulna	Humerus	Normal
Anterior hedgehog (20)	0	0	0	100% (20)
Mid-distal hedgehog (17)	41% (7)	17.5% (3)	11.5% (2)	41% (7)
$\beta$ -galactosidase (11)	0	0	0	100% (11)
Posterior hedgehog (7)	0	0	0	100% (7)

\*A single specimen might contribute to more than one column.

Percentage of grafts that induced extra skeletal elements (n)		
Graft (n)	Duplications	Normal
Hedgehog (46)	87% (40) <sup>†</sup>	13% (6)
$\beta$ -galactosidase (11)	0	100% (11)
Posterior hedgehog (7)	0	100% (7)

<sup>†</sup>38 specimens showed digit duplications.

QT6 cells transfected with either pCIS*Hhg-1* or pCIS*LacZ* were grafted to anterior, mid-distal or posterior borders of stage 20 chick limb buds. Embryos harvested at day 10 were fixed overnight in 10% formaldehyde, stained with Victoria Blue and cleared with methyl salicylate.

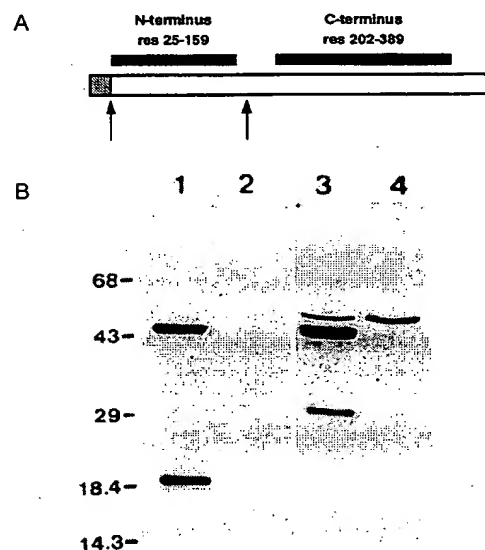


**Fig. 9. Proteolytic processing of the *Hhg-1* protein.** The filled boxes in A denote the portions of the *Hhg-1* ORF used to elicit antibodies, specific to the amino- and carboxy-terminal portions of the protein. The immunoblot in B illustrates the reactivity of amino-terminal (lanes 1 and 2) and carboxy-terminal (lanes 3 and 4) antibodies with species present in QT6 cells either transfected (lanes 1 and 3) or not transfected (lanes 2 and 4) with pCIS*Hhg-1*. Note the presence of a  $\sim 45 \times 10^3 M_r$  transfection-dependent species detected by both antibodies. Each antibody also detects a single smaller species of  $\sim 19 \times 10^3 M_r$  for the amino-terminal antibody and  $\sim 28 \times 10^3 M_r$  for the carboxy terminal antibody. The slightly larger species detected in lanes 3 and 4 is not transfection dependent, but provides a control for the amount of protein loaded. The arrows in A denote a signal cleavage (following the shaded hydrophobic domain) and a proposed internal cleavage that can account for the observed species and their reactivities (see text).

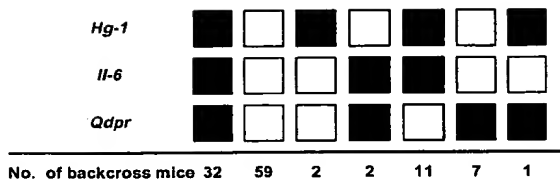


Fig. 10. Segregation of *Hhg-1* among proximal mouse chromosome 5 loci in [(C3H/HeJ-*gld* × *Mus spretus*)F<sub>1</sub> × C3H/HeJ-*gld*] interspecific backcross mice. Closed boxes represent the homozygous C3H pattern and open boxes the F<sub>1</sub> pattern. The number of mice with each haplotype is shown at the bottom of each column. The informative RFLV for *Hhg-1* is described in the text. The informative RFLVs for *Il-6* were generated by *TaqI* (C3H, 5.0 kb and 2.2 kb; *Mus spretus*, 8.6 kb and 1.9 kb) and for *Qdpr* were generated by *EcoRI* (C3H, 9.5 and 6.5 kb; *Mus spretus*, 8.2 kb).

large common species nor the smaller specific species are detected in untransfected cells (lanes 2 and 4). Essentially identical species were detected in protein extracts from heat shocked *Drosophila* embryos carrying the *hsHhg-1* construct, but not in extracts from unshocked embryos (D. T. C. and P. A. B., data not shown).

The arrows in Fig. 9A denote cleavages of the primary protein product that could account for *Hhg-1* species of the observed size. The first of these occurs at the *Hhg-1* signal sequence and is observed in a microsome-dependent fashion in *in vitro* translation reactions (J. J. Lee and P. A. B., unpublished data). The second internal cleavage is proposed as a simple possibility that can account for the observed polypeptide species and is similar to an internal cleavage that occurs in the *Drosophila hedgehog* protein precursor (J. J. Lee, S. C. Ekker and P. A. B., unpublished; see Discussion).

#### Chromosomal localization and fine mapping of *Hhg-1*

In order to determine the chromosomal location of the *Hhg-1* gene and to assess potential linkage with mouse developmental mutants, we analyzed a panel of DNA samples from an interspecific cross that has been characterized for over 500 genetic markers throughout the genome. The genetic markers included in this map span between 50 and 60 centi-Morgans (cMs) on each mouse autosome and on the X Chromosome (for examples see Saunders and Seldin, 1990; Watson et al., 1992). Initially, DNA from the two parental mice [C3H/HeJ-*gld* and (c3H/HeJ-*gld* × *Mus spretus*)F<sub>1</sub>] were digested with various restriction endonucleases and hybridized with *Hhg-1* cDNA probe to determine restriction fragment length variants (RFLVs) thereby allowing haplotype analyses. Informative RFLVs were detected with *MspI* restricted DNAs: C3H/HeJ-*gld*, 13.0 kb; *Mus spretus*, 5.0 kb. Comparison of the haplotype distribution of the *Hhg-1* indicated that in 109 of the 114 meiotic events examined, the *Hhg-1* locus cosegregated with *Il-6* (Fig. 10), a locus previously mapped to proximal mouse Chromosome 5 (Mock et al., 1989; Kozak and Stephenson, 1993). The best gene order (Bishop, 1985) ± the standard deviation (Green, 1981) indicated the following gene order from proximal to distal: *Hhg-1* – 4.4 cM ± 1.9 cM – *Il-6* – 15.7 cM ± 3.5 cM – *Qdpr*.

## DISCUSSION

### Patterning functions of *Hhg-1*

The most remarkable feature of *Hhg-1* expression, which has also been noted for other closely related genes in multiple vertebrate species (Riddle et al., 1993; Echelard et al., 1993; Krauss et al., 1993; Roelink et al., 1994), is its occurrence in a number of embryonic tissues demonstrated to exert patterning influences on neighboring structures. The notochord and floor plate, for example, are capable of imposing ventral pattern upon the neural tube (reviewed in Jessell and Dodd, 1993), while the posterior margin of the vertebrate limb bud or polarizing region can function as a posterior organizing center when grafted to a developing limb. Grafting experiments also suggest that these organizing activities may be functionally related, since notochord and floor plate tissue can also function as posterior organizing centers when grafted to limb buds (Wagner et al., 1990).

Riddle et al. (1993) indeed showed that the chicken *Shh* gene encodes a product capable of imposing pattern upon developing chick limbs while Echelard et al. (1993) showed that ectopic expression of chicken *Shh* can induce inappropriate expression of ventral neural tube markers in the mouse; Krauss et al. (1993) also showed that ectopic expression of fish *shh* can induce inappropriate expression of ventral neural tube markers in fish embryos. Finally, Roelink et al. (1994) demonstrated that COS cells expressing the rat gene *vhh-1* can induce formation of floor plate and motor neurons when cocultured with lateral neural tube explants from rat.

The xenoplastic activities of *Hhg-1* described here represent the first direct assays of function for the mouse member of the *vhh-1* or *sonic* class of vertebrate *hh*-like sequences. Our results also demonstrate for the first time the activity of a mammalian *hh*-like gene in limb patterning. Consistent with the expression of *Hhg-1* in the posterior margin of mouse limb buds, polarizing activity previously has been identified in this location by grafting experiments (Tickle et al., 1976; Fallon and Crosby, 1977). In addition, preliminary results in the explant assay system suggest that the *Hhg-1* product can also induce floor plate formation in rat lateral neural tube (J. Dodd, D. T. C. and P. A. B., unpublished data). We thus conclude that the *Hhg-1* gene encodes patterning activities and that the expression of pattern of *Hhg-1* in the embryo could account, at least in part, for the patterning activities of specific tissues assayed by grafting experiments.

A noteworthy feature of our grafting operations was the high relative frequency of proximal skeletal element duplications in mid-distal grafts (65%) versus anterior grafts (0%). Although such a correlation between graft location and the occurrence of proximal duplications has not been previously noted, a cursory review of the literature from the first polarizing region grafts of Saunders and Gasseling (1968) onwards suggests that graft location indeed appears to operate as a determinant for formation of proximal element duplications. More recently, Riddle et al. (1993) reported proximal element duplications induced by anterior grafts of cells expressing the chicken *Shh* gene. In both cases of proximal element duplication depicted, however, the digit sequence indicated a location sufficiently posterior to allow formation at least one digit anterior to the graft, thus reinforcing the correlation between proximal

element duplications and a more posterior graft location (at least as far posterior as mid-distal). The significance of this observation remains to be investigated.

### Genetic linkage of *Hhg-1*

Our segregation analysis of *Hhg-1* indicates a localization to the proximal region of mouse chromosome 5. Given the ability of *Hhg-1* to function in limb patterning, our attention was drawn to two mutations affecting limb development that also map to this region of mouse chromosome 5. One, *Hm* (hammertoe), is a semidominant mutation causing failure of normal programmed cell death in the webbing between toes during development, resulting in the formation of contractures in the second phalanx of all four limbs in the adult. This phenotype is somewhat more pronounced in homozygotes, which nevertheless remain viable and fertile. The second, *Hx* (Hemimelic extra toes), is also a dominant mutation associated with shortening or complete absence of tibia and talus in the hindlimbs and shortening of the radius in the forelimbs; in addition, metatarsals or metacarpals are duplicated giving a total of seven to eight digits per paw instead of the normal five (Dickie, 1968; Knudsen and Kochhar, 1981). The homozygous phenotype of *Hx* is an uncharacterized embryonic lethality (Knudsen and Kochhar, 1981). *Hx* and *Hm* are very closely linked but separate mutations, having been observed to recombine in only 1 of 3664 offspring from *trans*-heterozygous parents (Sweet, 1982). In addition to these mutations in the mouse, the syntenic region of human chromosome 7q has also been identified as the genetic locus for several developmental anomalies involving polydactyly (Tsukurov et al., 1994; Heutink et al., 1994).

In order to investigate the possibility that one or both of the mouse mutations affect the *Hhg-1* gene, we examined by Southern blotting the restriction pattern of DNA from both of these mutants. Using nine different restriction endonucleases for *Hx* and for *Hm*, we detected no differences between parental and mutant DNA (data not shown). Since the *Hx* phenotype suggests a defect in early limb patterning, as might be expected from a mutation in the *Hhg-1* gene, we attempted to discover alterations in *Hhg-1* coding sequences in the *Hx* mutant. Because only heterozygous *Hx* mutant DNA was available (from Jackson Labs), our conclusions depend upon analysis of multiple independently isolated clones. We examined eleven, fourteen and eight independent clones from the coding portions of exons one, two and three, respectively, without detecting any differences from wild type (see Materials and Methods). Since the clones for sequence determination were derived using the polymerase chain reaction, it is possible that a deletion(s) at the *Hhg-1* locus might have prevented amplification of the mutant allele. Given the uncertainty inherent in sampling from heterozygous DNA, it is also formally possible, although highly unlikely, that we could have missed a coding difference in the *Hhg-1* gene of *Hx* mutants.

In the absence of *Hx*- or *Hm*-associated alterations in *Hhg-1* coding sequence, another possibility to consider is that the *Hx* or *Hm* phenotypes could result from a mutation in *cis*-acting regulatory regions of *Hhg-1*, causing either a reduction of *Hhg-1* expression or inappropriate spatial localization of expression. Given our Southern blotting results, such a lesion could lie near the *Hhg-1* gene only if it is sufficiently subtle to escape detection by Southern blotting with our cDNA probe;

alternatively, a *Hhg-1* regulatory lesion may have escaped detection because of a location distant from sequences represented within the *Hhg-1* cDNA.

With regard to potential mechanisms underlying genetic dominance for such a regulatory mutation, the dominant limb deformity mutation *Xt* (extra toes) may be informative. Like *Hx*, *Xt* causes polydactyly and is lethal when homozygous; mutations affect the gene *GLI3*, which encodes a zinc finger transcription factor. At least one allele of *Xt* appears to act simply by disrupting transcription of *GLI3* (Schimmang et al., 1992), and thus, the genetic dominance of mutations at this locus is probably due to haploinsufficiency. The *GLI3* gene is also interesting in that its close *Drosophila* relative, the gene *cubitus-interruptus*<sup>Dominant</sup> (*ci<sup>D</sup>*), functions downstream in the *hedgehog* signaling pathway (Forbes et al., 1993). If the *GLI3* gene similarly functions downstream of *Hhg-1* in the mouse, and given that *GLI3* function is haploinsufficient, it would not be surprising to find that partial loss of *Hhg-1* expression caused by a regulatory mutation might also have a dominant phenotype. Interestingly, a human polysyndactyly disease that maps to a region of human chromosome 7 syntenic to the region containing *Hhg-1* and *Hm* and *Hx* is also inherited in a dominant fashion (Tsukurov et al., 1994; Heutink et al., 1994). Alternatives to haploinsufficiency are that a regulatory mutation might cause *Hhg-1* mis-expression or that *Hx* and *Hm* are unrelated to *Hhg-1*.

### Duplication and divergence of the *hedgehog* gene family in vertebrates

Our PCR-based search for vertebrate *hedgehog* homologues yielded the three distinct mouse and two distinct human sequences reported here, and five sequences each from the zebrafish *Brachydanio rerio* and the toad *Xenopus laevis* (S. C. Ekker, J. J. Lee, D. v. K. and P. A. B., unpublished data). In contrast, none of the invertebrate species to which our PCR-based method was applied yielded more than a single distinct *hh*-like sequence. For example, using various combinations of degenerate primers from conserved regions, eighteen independent *Drosophila melanogaster* clones identical to *hh* were isolated without encountering any diverged *hh*-like sequences. It is not yet possible to estimate accurately the total number of distinct vertebrate *hh*-like genes. The occurrence of multiple *hh*-like sequences in vertebrates but not invertebrates nevertheless suggests that at some point during evolution of the vertebrate lineage repeated duplication and divergence of a single ancestral *hedgehog* gene occurred, as has been proposed for the origin of multiple vertebrate HOM-C gene clusters from a single ancestral cluster (Schubert et al., 1993).

### Broad evolutionary conservation of *hedgehog* protein function and proteolytic processing

The evolutionary conservation of *hh* extends beyond sequence to include function, as demonstrated by the ability of *Hhg-1* to encode a signal capable of inducing expansion of the *wingless* stripe of expression in *Drosophila* embryos. Similar results using a *hh*-like gene isolated from zebrafish were also reported by Krauss et al. (1993). If the proposal, based on genetic arguments, that the gene *patched* (*ptc*) encodes a *hh* receptor in *Drosophila* is correct (Ingham et al., 1991), the functional conservation of vertebrate *hedgehog* signals would suggest that *ptc*-like sequences and function should also be conserved in



vertebrates. With regard to the identity of a *hh* receptor, however, we observed that both *hh* and *Hhg-1* can induce broadening of the *wingless* stripe when ectopically expressed at the retracted germ band stage of *Drosophila* development. By this stage, the initially broad stripe of *ptc* mRNA and protein expression has split into two thinner stripes per segment by loss of expression from the cells in the middle of the broad stripe (Taylor et al., 1993). Expanded *wingless* expression in response to *hh* thus is occurring in interstripe cells that in normal embryos no longer express the *ptc* protein. Ingham (1993) has reported that *ptc* expression in these interstripe cells is also induced by ectopic *hedgehog*, but it is not known whether *ptc* induction in the interstripe precedes or follows *wg* induction in the interstripe cells. Whatever the sequence of induction, novel expression of *ptc* or *wg* represents a response to *hh* protein in interstripe cells, which do not express the *ptc* protein, thus suggesting that *ptc* does not encode the *hh* receptor, or at least not the only receptor.

The occurrence of multiple *Hhg-1* polypeptide species in *Drosophila* embryos as well as in avian cells raises a question as to the role of proteolytic processing in *hedgehog* protein function. We believe that the N- and C-terminally derived forms of the *Hhg-1* protein bear a product/precursor relationship to the larger form because the relative molecular masses of the smaller products sum to yield approximately the relative molecular mass of the larger product, and they could therefore be derived by a single internal cleavage as shown in the model in Fig. 9A. The location of this internal cleavage coincides approximately with an intron/exon boundary and with a sharp demarcation in the degree of sequence conservation (see Results). In addition, these smaller forms resemble smaller forms of the *hh* protein observed in *Drosophila* (Tabata and Kornberg, 1994; J. J. Lee and P. A. B., unpublished data), where an internal cleavage occurs and appears to be required for the *hh* signaling function (J. J. Lee, S. C. Ekker, D. P. von K. and P. A. B., unpublished data).

The existence of two distinct stable products derived from a single larger precursor may provide a clue to the apparent dual nature of *hedgehog* gene action in several developmental systems. In the *Drosophila* embryo, for example, the restriction of *wingless* gene expression to a narrow stripe within each segment is dependent upon the short-range nature of a *hedgehog* signaling activity (see above; Ingham, 1993); in contrast, the influence of a later-acting *hh*-encoded activity extends across most of the segment in imposing pattern upon the dorsal cuticle (Heemskerk and DiNardo, 1994). Similarly in ventral neural tube patterning, induction of floor plate occurs at short range and depends upon direct contact with notochord, floor plate, or COS cells expressing *vhh-1* (Placzek et al., 1993; Roelink et al., 1994). COS cells expressing *vhh-1* also have motor neuron inducing activity (Roelink et al., 1994). This latter activity is found in diffusible form in supernatants from notochord and floor plate cultures (Yamada et al., 1993), although it is not yet clear that *vhh-1* directly encodes the diffusible activity. Long- and short-range *hedgehog* activities have not been definitively identified in the context of limb patterning, but such activities have been extensively discussed; dual modes of *hedgehog* action thus may yet emerge from studies of such apparently distinct activities as influences upon the apical ectodermal ridge and anterior/posterior patterning of the developing limb.

An alternative would be that only one of the smaller *hedgehog* protein species is biologically active, with the apparent dual nature of *hedgehog* action deriving from secondary effects. For example, restricted diffusion for the primary active species could produce apparent long-range effects by inducing expression of another diffusible molecule. Similarly, a diffusible or primarily long-range *hedgehog* signal could yield apparent short-range effects through threshold-dependent responses of target cells. To resolve these questions, the structures and embryonic localizations of the *hedgehog*-encoded proteins must be determined and their patterning activities assayed. At another level, a true understanding of the functional roles of vertebrate *hedgehog* proteins requires a demonstration that patterning functions in vertebrate embryos actually are executed by the products of this class of genes; this would best be achieved through specific inactivation of *hedgehog* gene products by genetic or other means.

We gratefully acknowledge J. Gearhart, S.-J. Lee, C. Moore, C. Mjaatvedt and T. Huynh for instruction in handling of mice, manipulation of embryos, and advice on in situ hybridisation. We also thank A. Lanahan, J. Williams and S.-J. Lee for mouse cDNA libraries and RNA blots, K. Young, M. Claudia, D. Sullivan, J. Kassis, S. Brown, R. Denell, G. Aisenberg and A. Cameron generously provided genomic DNA and libraries from various species, and K. Young graciously assisted in the isolation and characterization of the mosquito and mouse sequences. We are indebted to N. Patel for equipment and help with dark field microscopy. We also thank J. Dodd, J. J. Lee and S. C. Ekker, for sharing unpublished data, and S. C. Ekker for help with figures. T. Vogt and S.-J. Lee provided useful comments on the manuscript. This work was supported by the Howard Hughes Medical Institute, an NIH MSTP award to D. T. C., NIH awards HD20743 and 5T32GM07507 to J. F. F. and A. L., and NIH award HG00734 to M. F. S.

## REFERENCES

- Ausubel, F. M., Brent, R., Kingston, R. E., Moore, D. D., Seidman, J. G., Smith, J. A. and Struhl, K. (1993). *Current Protocols in Molecular Biology*. New York: Greene Publishing Associates and Wiley-Interscience.
- Baker, N. E. (1988). Embryonic and imaginal requirements for *wingless*, a segment polarity gene in *Drosophila*. *Dev. Biol.* 125, 96-108.
- Bejsovec, A. and Martinez-Arias, A. (1991). Roles of *wingless* in patterning the larval epidermis of *Drosophila*. *Development* 113, 471-485.
- Bejsovec, A. and Wieschaus, E. (1993). Segment polarity gene interactions modulate epidermal patterning in *Drosophila* embryos. *Development* 119, 501-517.
- Bishop, D. T. (1985). The information content of phase-known matings for ordering genetic loci. *Genet. Epidemiol.* 2, 349-361.
- Burnette, W. N. (1981). Western blotting: electrophoretic transfer of proteins from sodium dodecyl sulfate-polyacrylamide gels to unmodified nitrocellulose and radiographic detection with antibody and radio-iodinated Protein A. *Anal. Biochem.* 112, 195-203.
- Chen, C. and Okayama, H. (1987). High-efficiency transformation of mammalian cells by plasmid DNA. *Molecular & Cellular Biology* 7, 2745-2752.
- Dickie, M. M. (1968). *Mouse News Lett.* 38, 24.
- DiNardo, S., Sher, E., Heemskerk-Jongens, J., Kassis, J. A. and O'Farrell, P. H. (1988). Two-tiered regulation of spatially patterned *engrailed* gene expression during *Drosophila* embryogenesis. *Nature* 332, 604-609.
- Dougan, S. and DiNardo, S. (1992). *Drosophila wingless* generates cell type diversity among *engrailed* expressing cells. *Nature* 360, 347-50.
- Echelard, Y., Epstein, D. J., St-Jacques, B., Shen, L., Mohler, J., McMahon, J. A. and McMahon, A. P. (1993). Sonic hedgehog, a member of a family of putative signaling molecules, is implicated in the regulation of CNS polarity. *Cell* 75, 1417-1430.
- Fallon, J. F. and Crosby, G. M. (1977). Polarizing zone activity in limb buds

- of amniotes. In *Vertebrate Limb and Somite Morphogenesis*. (ed. D. A. Ede, J. R. Hinchliffe and M. Balls), pp 55-70. Cambridge: England.
- Feinberg, A. and Vogelstein, B. (1983). A technique for radiolabeling DNA restriction endonuclease fragments to high specific activity. *Anal. Biochem.* **132**, 6-13.
- Ferguson, E. L. and Anderson, K. V. (1992). Decapentaplegic acts as a morphogen to organize dorsal-ventral pattern in the *Drosophila* embryo. *Cell* **71**, 451-461.
- Forbes, A. J., Nakano, Y., Taylor, A. M. and Ingham, P. W. (1993). Genetic analysis of *hedgehog* signalling in the *Drosophila* embryo. *Development* **193** Supplement, 115-124.
- Gorman, C. (1985). High efficiency gene transfer into mammalian cells. In *DNA cloning*. (ed. D. M. Glover), pp 143. Oxford.
- Green, E. L. (1981). Linkage, recombination and mapping. In *Genetics and Probability in Animal Breeding Experiments*. (ed. E. Green), pp 77-113. New York.
- Harlow, E. and Lane, D. (1988). *Antibodies: A Laboratory Manual*. Cold Spring Harbor, New York: Cold Spring Harbor Publications.
- Heberlein, U., Wolff, T. and Rubin, G. M. (1993). The TGF beta homolog *dpp* and the segment polarity gene *hedgehog* are required for propagation of a morphogenetic wave in the *Drosophila* retina. *Cell* **75**, 913-926.
- Heemskerk, J. and DiNardo, S. (1994). *Drosophila hedgehog* acts as a morphogen in cellular patterning. *Cell* **76**, 449-460.
- Heutink, P., Zguricas, J., Oosterhout, L. v., Breedveld, G. J., Testers, L., Sandkuijl, L. A., Snijders, P. J. L. M., Weissenbach, J., Lindhout, D., Hovius, S. E. R. and Oostra, B. A. (1994). The gene for triphalangeal thumb maps to the subtelomeric region of chromosome 7q. *Nature Genetics* **6**, 287-292.
- Ingham, P. W. (1993). Localized *hedgehog* activity controls spatial limits of wingless transcription in the *Drosophila* embryo. *Nature* **366**, 560-562.
- Ingham, P. W., Taylor, A. M. and Nakano, Y. (1991). Role of the *Drosophila patched* gene in positional signalling. *Nature* **353**, 184-187.
- Jessell, T. M. and Dodd, J. (1993). Control of neural cell identity and pattern by notochord and floor plate signals. In *Cell-Cell Signaling in Vertebrate Development*. (ed. E. J. Robertson, F. R. Maxfield and H. J. Vogel), pp 139-155. San Diego.
- Knudsen, T. B. and Kochhar, D. M. (1981). The role of morphogenetic cell death during abnormal limb-bud outgrowth in mice heterozygous for the dominant mutation *Hemimelia-extra toe* (*Hmx*). *J. Embryol. Exp. Morphol.* **65** (Supplement), 289-307.
- Kozak, C. A. and Stephenson, D. A. (1993). Mouse chromosome 5. *Mammalian Genome* **4**, 572-87.
- Krauss, S., Concordet, J.-P. and Ingham, P. W. (1993). A functionally conserved homolog of the *Drosophila* segment polarity gene *hh* is expressed in tissues with polarizing activity in zebrafish embryos. *Cell* **75**, 1431-1444.
- Laemmli, U. K. (1970). Cleavage of structural proteins during the assembly of the head of bacteriophage T4. *Nature* **227**, 680-685.
- Lee, J. J., von Kessler, D. P., Park, S. and Beachy, P. A. (1992). Secretion and localized transcription suggest a role in positional signaling for products of the segmentation gene *hedgehog*. *Cell* **71**, 33-50.
- Lee, S. J. (1990). Identification of a novel member (GDF-1) of the transforming growth factor- $\beta$  superfamily. *Mol. Endocrinol.* **4**, 1034-1040.
- Lockyer, J., Cook, R. G., Milatien, S., Kaufman, S., Woo, S. L. C. and Ledley, F. D. (1987). Structure and expression of human dihydropteridine reductase. *Proc. Natl. Acad. Sci. USA* **84**, 3329-3333.
- Ma, C., Zhou, Y., Beachy, P. A. and Moses, K. (1993). The segment polarity gene *hedgehog* is required for progression of the morphogenetic furrow in the developing *Drosophila* eye. *Cell* **75**, 927-938.
- Martinez Arias, A., Baker, N. E. and Ingham, P. W. (1988). Role of segment polarity genes in the definition and maintenance of cell states in the *Drosophila* embryo. *Development* **103**, 157-170.
- Mock, B. A., Nordan, R. P., Justice, M. J., Kozak, C., Jenkins, N. A., Copeland, N. G., Clark, S. C., Wong, G. G. and Rudnikoff, S. (1989). The murine *Il-6* gene maps to the proximal region of Chromosome 5. *Journal of Immunology* **142**, 1372-1376.
- Mohler, J. (1988). Requirements for *hedgehog*, a segmental polarity gene, in patterning larval and adult cuticle of *Drosophila*. *Genetics* **120**, 1061-1072.
- Mohler, J. and Vani, K. (1992). Molecular organization and embryonic expression of the *hedgehog* gene involved in cell-cell communication in segmental patterning in *Drosophila*. *Development* **115**, 957-971.
- Moscovici, C., Moscovici, M. G., Jimenez, H., Lai, M. M., Hayman, M. J. and Vogt, P. K. (1977). Continuous tissue culture cell lines derived from chemically induced tumors of Japanese quail. *Cell* **11**, 95-103.
- Nusse, R. and Varmus, H. E. (1992). *Wnt* genes. *Cell* **69**, 1073-1087.
- Peifer, M. and Bejsovec, A. (1992). Knowing your neighbors: cell interactions determine intrasegmental patterning in *Drosophila*. *Trends in Genetics* **8**, 243-249.
- Placzek, M., Jessell, T. M., and Dodd, J. (1993). Induction of floor plate differentiation by contact-dependent homeogenetic signals. *Development* **117**, 205-218.
- Riddle, D. R., Johnson, R. L., Laufer, E. and Tabin, C. (1993). Sonic hedgehog mediates the polarizing activity of the ZPA. *Cell* **75**, 1401-1416.
- Rijsewijk, F., Schuermann, M., Wagenaar, E., Parren, P., Weigel, D. and Nusse, R. (1987). The *Drosophila* homolog of the mouse mammary oncogene *int-1* is identical to the segment polarity gene *wingless*. *Cell* **50**, 649-657.
- Riley, B. B., Savage, M. P., Simandl, B. K., Olwin, B. B. and Fallon, J. F. (1993). Retroviral expression of FGF-2 (bFGF) affects patterning in chick limb bud. *Development* **118**, 95-104.
- Roelink, H., Augsburger, A., Heemskerk, J., Korzh, V., Norlin, S., Ruiz i Altaba, A., Tanabe, Y., Placzek, M., Edlund, T., Jessell, T. M. and Dodd, J. (1994). Floor plate and motor neuron induction by *vhh-1*, a vertebrate homolog of *hedgehog* expressed by the notochord. *Cell* **76**, 761-775.
- Rubin, G. M. and Spradling, A. C. (1982). Genetic transformation of *Drosophila* with transposable element vectors. *Science* **218**, 348-353.
- Sambrook, J., Fritsch, E. F. and Maniatis, T. (1989). *Molecular Cloning: A Laboratory Manual*. 2nd edition Cold Spring Harbor, Cold Spring Harbor Laboratory Publications.
- Sanger, F., Nicklen, S. and Coulson, A. R. (1977). DNA sequencing with chain-terminating inhibitors. *Proc. Natl. Acad. Sci. USA* **74**, 5463-5467.
- Saunders, A. M. and Seldin, M. F. (1990). A molecular genetic linkage map of mouse chromosome 7. *Genomics* **8**, 524-535.
- Saunders, J. W. and Gasseling, M. (1968). Ectodermal-mesenchymal interaction in the origin of limb symmetry. In *Epithelial-Mesenchymal Interaction*. (ed. R. Fleischmayer and R. E. Billingham), pp 78-97. Baltimore.
- Schimmgang, T., Lemaistre, M., Vortkamp, A. and Ruther, U. (1992). Expression of the zinc finger gene *Gli3* is affected in the morphogenetic mouse mutant *extra-toes* (*Xt*). *Development* **116**, 799-804.
- Schubert, F. R., Nieselt-Struwe, K. and Gruss, P. (1993). The Antennapedia-type homeobox genes have evolved from three precursors separated early in metazoan evolution. *Proc. Natl. Acad. Sci. USA* **90**, 143-147.
- Seldin, M. F., Morse, H. C., Reeves, J. P., Scribner, J. P., LeBoeuf, R. C. and Steinber, A. D. (1988). Genetic analysis of autoimmune *gld* mice 1. Identification of a restriction fragment length polymorphism closely linked to the *gld* mutation within a conserved linkage group. *J. Exp. Med.* **167**, 688-693.
- Sweet, H. O. (1982). *Mouse News Lett.* **66**, 66.
- Tabata, T., Eaton, S. and Kornberg, T. (1992). The *Drosophila hedgehog* gene is expressed specifically in posterior compartment cells and is a target of engrailed regulation. *Genes Dev.* **6**, 2635-2645.
- Tabata, T. and Kornberg, T. B. (1994). *Hedgehog* is a signaling protein with a key role in patterning *Drosophila* imaginal discs. *Cell* **76**, 89-102.
- Tashiro, S., Michiue, T., Higashijima, S., Zenno, S., Ishimaru, S., Takahashi, F., Orihara, M., Kojima, T. and Saigo, K. (1993). Structure and expression of *hedgehog*, a *Drosophila* segment polarity gene required for cell-cell communication. *Gene* **124**, 183-189.
- Tautz, D. and Pfeifle, C. (1989). A non-radioactive *in situ* hybridization method for the localization of specific RNAs in the *Drosophila* embryo reveals translational control of the segmentation gene *hunchback*. *Chromosoma* **98**, 81-85.
- Taylor, A. M., Nakano, Y., Mohler, J. and Ingham, P. W. (1993). Contrasting distributions of *patched* and *hedgehog* proteins in the *Drosophila* embryo. *Mech. Dev.* **42**, 89-96.
- Thummel, C. S., Boulet, A. M. and Lipshitz, H. D. (1988). Vectors for *Drosophila* P-element-mediated transformation and tissue culture transfection. *Gene* **74**, 445-456.
- Tickle, C., Shellswell, G., Crawley, A. and Wolpert, L. (1976). Positional signalling by mouse limb polarising region in the chick wing bud. *Nature* **259**, 396-397.
- Tsukurov, O., Boehmer, A., Flynn, J., Nicolai, J.-P., Hamel, B. C. J., Traill, S., Zaleske, D., Mankin, H. J., Yeon, H., Ho, C., Tabin, C., Seidman, J. G. and Seidman, C. (1994). A complex bilateral polysyndactyly disease locus maps to chromosome 7q36. *Nature Genetics* **6**, 282-286.
- von Heijne, G. (1986). A new method for predicting signal sequence cleavage sites. *Nucl. Acids Res.* **14**, 4683-4690.
- Wagner, M., Thaller, C., Jessell, T. and Eichele, G. (1990). Polarizing activity and retinoid synthesis in the floor plate of the neural tube. *Nature* **345**, 819-822.

- Watson, M. L., D'Eustachio, P. D., Mock, B. A., Steinberg, A. D., Morse, H. C. I., Oakey, R. J., Howard, T. A., Rochelle, J. M. and Seldin, M. F. (1992). A linkage map of mouse chromosome 1 using an interspecific cross segregating for the *gld* autoimmunity mutation. *Mammalian Genome* 2, 158-171.
- Wieschaus, E. and Nusslein-Volhard, C. (1986). Looking at embryos. In *Drosophila: A Practical Approach*. (ed. D. B. Roberts), pp 199-227. Oxford: England.
- Wilkinson, D. G. (1992). Whole mount *in situ* hybridization of vertebrate embryos. In *In situ hybridization: A practical approach*. (ed. D. G. Wilkinson), pp 75-83. Oxford.
- Wolpert, L. (1969). Positional information and the spatial pattern of cellular differentiation. *Journal of Theoretical Biology* 25, 1-47.
- Yamada, T., Pfaff, S. L., Edlund, T., and Jessell, T. M. (1993). Control of cell pattern in the neural tube: motor neuron induction by diffusible factors from notochord and floor plate. *Cell* 73, 673-686.

(Accepted 12 August 1994)

# The morphogen Sonic hedgehog is an indirect angiogenic agent upregulating two families of angiogenic growth factors

ROBERTO POLA<sup>1</sup>, LEONA E. LING<sup>2</sup>, MARCY SILVER<sup>1</sup>, MICHAEL J. CORBLEY<sup>2</sup>, MARIANNE KEARNEY<sup>1</sup>,  
R. BLAKE PEPINSKY<sup>2</sup>, RENEE SHAPIRO<sup>2</sup>, FREDERICK R. TAYLOR<sup>2</sup>, DARREN P. BAKER<sup>2</sup>,  
TAKAYUKI ASAHARA<sup>1</sup> & JEFFREY M. ISNER<sup>1</sup>

<sup>1</sup>Department of Medicine, St. Elizabeth's Medical Center,  
Tufts University School of Medicine, Boston, Massachusetts, USA

<sup>2</sup>Biogen Incorporated, Cambridge, Massachusetts, USA

R.P. and L.E.L. contributed equally to this study.

Correspondence should be addressed to J.M.I.; email: [vejeff@aol.com](mailto:vejeff@aol.com)

Sonic hedgehog (Shh) is a prototypical morphogen known to regulate epithelial/mesenchymal interactions during embryonic development. We found that the hedgehog-signaling pathway is present in adult cardiovascular tissues and can be activated *in vivo*. Shh was able to induce robust angiogenesis, characterized by distinct large-diameter vessels. Shh also augmented blood-flow recovery and limb salvage following operatively induced hind-limb ischemia in aged mice. *In vitro*, Shh had no effect on endothelial-cell migration or proliferation; instead, it induced expression of two families of angiogenic cytokines, including all three vascular endothelial growth factor-1 isoforms and angiopoietins-1 and -2 from interstitial mesenchymal cells. These findings reveal a novel role for Shh as an indirect angiogenic factor regulating expression of multiple angiogenic cytokines and indicate that Shh might have potential therapeutic use for ischemic disorders.

Hedgehog (Hh) proteins act as morphogens in many tissues during embryonic development<sup>1-6</sup>. The mature forms of Hh are 19-kD proteins that interact with heparin through an N-terminal basic domain and are tethered to the cell membrane through cholesterol and fatty acyl modification<sup>9-11</sup>. Hh acts upon mesoderm in epithelial-mesenchymal interactions that are crucial to the formation of limb, lung, gut, hair follicles and bone<sup>2-6</sup>. Among the three highly conserved mammalian Hh genes, Sonic hedgehog (Shh) is the most widely expressed during development<sup>12,13</sup> and Shh deficiency in mice is embryonically lethal leading to multiple defects beginning in early to mid gestation<sup>13-5</sup>. Indian hedgehog (Ihh) is less widely expressed and Ihh-deficient mice survive to late gestation with skeletal and gut defects<sup>4,6,13</sup>. Desert hedgehog (Dhh) is expressed in the peripheral nerves, male gonads, as well as the endothelium of large vessels during development<sup>13</sup>. Dhh-deficient mice are viable but have peripheral-nerve and male-fertility defects<sup>7,8</sup>.

Hh signaling occurs through the interaction of Hh protein with its receptor, Patched-1 (Ptc1 encoded by *Ptc1*)<sup>14</sup>. This leads to activation of a transcription factor, Gli, which induces expression of downstream target genes including *Ptc1* and *Gli* themselves<sup>15-23</sup>. Thus Ptc1 and Gli are both required components as well as transcriptionally induced targets of the Hh signaling pathway.

Several recent observations point to the involvement of Hh in vascularizing certain embryonic tissues. First, hypervascularization of neuroectoderm is seen following transgenic overexpression of Shh in the dorsal neural tube<sup>24</sup>. Second, Shh-deficient zebrafish exhibits disorganization of endothelial precursors and an inability to form the dorsal aorta or axial vein<sup>25</sup>. Third, Shh-deficient mice lack proper vascularization of the developing lung<sup>3</sup>. Fourth, Ihh, expressed by prehypertrophic chondrocytes, regulates the rate of chondrocyte maturation, a process closely

correlated to the induction of angiogenesis in bone<sup>26,27</sup>. Finally, the induction of anagen in the hair follicle requires both Shh and angiogenesis<sup>28,29</sup>. Although these findings implicate the Hh pathway in vascular development, it is not clear whether these effects are due to a direct angiogenic action of Hh.

Here, we used postnatal mouse models to directly test the impact of Shh on vascularization *in vivo*. We show that cells in the adult cardiac and vascular tissues express Ptc1 and can respond to exogenous Hh by Ptc1 overexpression. In addition, we tested the angiogenic properties of Shh in the corneal and ischemic hind-limb models of angiogenesis. We found that Shh is a potent angiogenic factor, and when administered to aged mice it is able to induce robust neovascularization of ischemic hind-limbs. Shh-induced angiogenesis is characterized by large-diameter vessels. Investigation of the mechanism responsible for these findings established that Shh is an indirect angiogenic agent, inducing up-regulation of two families of angiogenic growth factors, including vascular endothelial growth factor (VEGF) and the angiopoietins Ang-1 and Ang-2. Our data indicate a novel and unexpected biological activity for Hh with potential therapeutic implications.

## Hh signaling in postnatal vasculature

In juvenile and adult mice, we found that Ptc1 is normally expressed in cardiovascular tissues (Fig. 1). We visualized Ptc1 expression using  $\beta$ -galactosidase ( $\beta$ -gal) staining of vascular tissues from mice that have a non-disruptive insertion of a nuclear localization signal (NLS)-tagged *lacZ* reporter gene upstream of the *Ptc1* coding region (NLS-*Ptc1-lacZ* mice). Ptc1 expression corresponds to *lacZ* expression in postnatal tissues and does not appear to be altered by *lacZ* insertion (L. Ling, unpublished observations). When examined for nuclear  $\beta$ -gal expression, NLS-*Ptc1-lacZ* mice exhibited basal Ptc1 expression in adventitial cells,

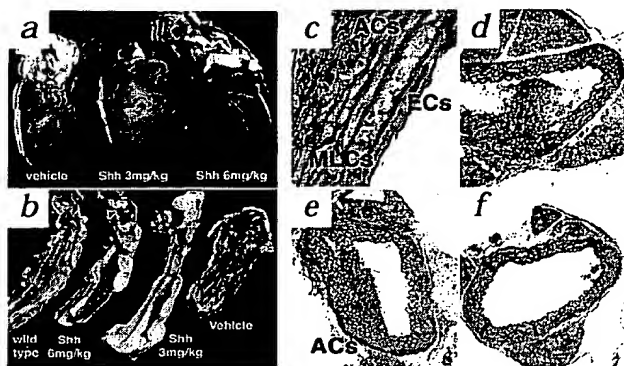


**Fig. 1** *Ptc* expression and activation in postnatal cardiovascular tissues. **a** and **b**, Hearts (**a**) and aortas (**b**) from NLS-*Ptc-lacZ*. Vehicle-treated mice exhibit a basal level of *Ptc* expression; administration of Shh result in a dose-dependent increase in *Ptc* expression in both hearts and aortas. **c** and **d**, Paraffin cross sections from vehicle-treated mice (**c**) or untreated (**d**) mice show *Ptc* expression in endothelial cells (ECs), medial layer cells (MLCs) and adventitial cells (ACs). **e** and **f**, Treatment with Shh (**e**) increases *Ptc* expression in adventitial cells. Aortas from wild-type littermates treated with Shh show no *Ptc* expression (**f** and **g**). Magnification **c**,  $\times 200$ ; **d-f**,  $\times 100$ .

endothelial cells and cells in the medial layer of the vasculature (Fig. 1c). These results indicated that adult cardiovascular tissues have several resident populations of cells that might be responsive to Hh. To test this hypothesis, day 6 postnatal NLS-*Ptc-lacZ* mice were injected subcutaneously with Shh once daily for three days. This treatment induced a dose-dependent increase in *Ptc* expression in coronary arteries and aortas (Fig. 1a, b and e). In particular, adventitial cells showed a significant increase in *Ptc* expression (Fig. 1e). These cells were vimentin-positive, consistent with aortic adventitial fibroblasts (data not shown).

#### Shh induces vascular growth and promotes limb salvage

We tested the potential for Shh to act upon the adult vasculature and protect against ischemic injury by administering Shh, the VEGF-1 isoform recombinant human (rh)VEGF<sub>165</sub> or control to aged mice undergoing unilateral, surgically induced hind-limb ischemia. Aged mice have impaired angiogenesis, decreased blood-flow recovery, and typically develop limb necrosis from ischemic injury due to an inherent compromise in endogenous neovascularization<sup>30</sup>. A blinded evaluation showed that two-year-old mice receiving control developed profound consequences of hind-limb ischemia (including auto-amputation and foot/leg necrosis): 65% at day 7 after surgery, 73% at day 14, 80% at day 21, and 82% at day 28 (Fig. 2a). Similarly, mice treated with intramuscular injections of rhVEGF<sub>165</sub> had severe necrosis or auto-amputation of the ischemic limb comparable to vehicle-treated mice (data not shown). In contrast, we observed a sharp increase in limb salvage in mice treated with Shh. In this group,

the percentage of auto-amputated limbs and foot/leg necrosis decreased to 25% at day 7 after surgery, 47% at day 14, 50% at day 21, and 50% at day 28 (Fig. 2a). Complete limb salvage after 21 and 28 days follow-up was obtained in half of the mice treated with Shh compared with less than 20% in the vehicle and rhVEGF<sub>165</sub>-treated groups.

Laser power doppler imaging (LDPI) performed independently by two blinded operators demonstrated a progressive increase in the blood flow of ischemic hind limbs in Shh-treated mice, with significant differences seen at day 28 ( $P < 0.01$ ) (Fig. 2b). In contrast, we observed no significant increase in hind-limb perfusion beyond 28 days of follow-up in control mice. At day 28 after surgery, the Doppler flow ratio was significantly increased in Shh-treated mice in comparison to the groups treated with rhVEGF<sub>165</sub> or vehicle ( $P < 0.05$ ) (Fig. 2b and data not shown).

Likewise, capillary density at day 28 after surgery was significantly increased in Shh-treated versus rhVEGF<sub>165</sub>- and control-treated mice ( $P < 0.001$  and  $P < 0.0001$ , respectively) (Fig. 2c, d and data not shown). Neovascularization induced by Shh was characterized not only by increased numbers of capillaries, but also by a substantial increase in vessel diameter (Fig. 2d).

#### Shh-induced angiogenesis has distinctive morphology

To determine the basis of augmented neovascularization in response to Shh, we used the murine corneal angiogenesis model. We implanted pellets containing Shh and/or VEGF, or control in the corneas of 8–12-week-old C57BL/6J mice. Six days after implantation, both VEGF- and Shh-treated eyes exhibited growth of neovessels whereas none induced by control pellets (Fig. 3a, b and c). Whole-mount fluorescent BS1 lectin (*Bandeiraea simplicifolia* lectin-1, an endothelial cell marker) staining and CD31 immunostaining of cross sections showed several striking differences in morphology between Shh-induced neovessels and those induced by VEGF. Consistent with the previous observations in the is-

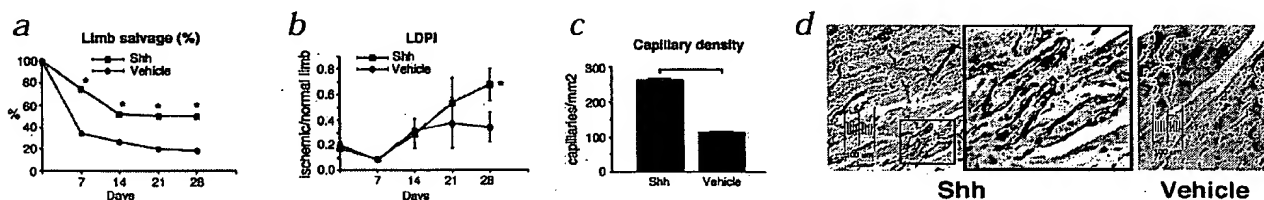
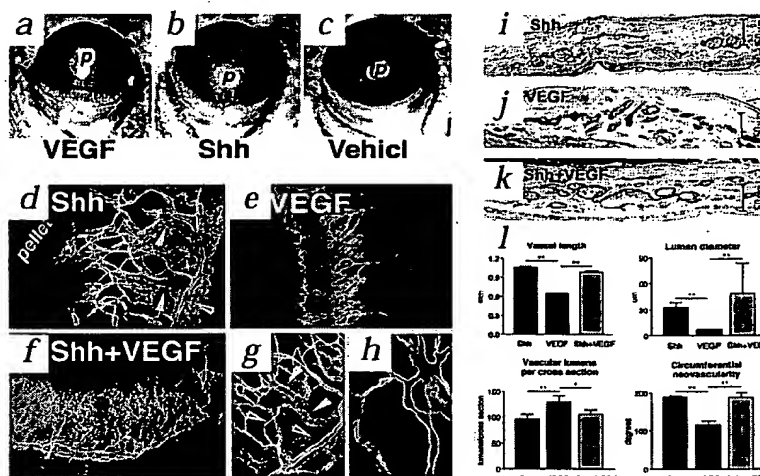


**Fig. 2** Shh increases limb salvage, blood flow and capillary density in the setting of ischemia. **a**, Limb salvage: at each time point, the percentage of limb salvage is statistically significantly higher in Shh-treated group (■) compared with vehicle (●). \*,  $P < 0.05$ . **b**, Blood flow: ischemic/normal leg perfusion ratio is extremely low in both groups immediately after surgery, but progressively increases over time in Shh-treated mice (■), achieving significant improvement by day 28. \*,  $P < 0.01$ . In contrast, no increase in hind-limb perfusion was seen over

time in mice treated with vehicle (●). Ischemic/normal leg perfusion ratio at day 28 is significantly higher in Shh-treated mice compared with vehicle ( $0.681 \pm 0.126$  versus  $0.344 \pm 0.119$ ;  $P < 0.05$ ). **c**, Capillary density at day 28 after surgery is significantly increased in mice treated with Shh compared with vehicle ( $P < 0.0001$ ). **d**, Representative pictures of capillary density show that the number of vessels is increased in Shh-treated tissues. A higher magnification ( $\times 400$ ) of Shh-treated skeletal muscle (middle) shows a substantial increase in vessel diameter.

**Fig. 3** Shh-induced angiogenesis has unusual morphological characteristics. **a–c**, Neovascular growth is detectable in corneas implanted with pellets ('p') containing VEGF (**a**) and Shh (**b**), but not vehicle (**c**). **d–h**, Shh (**d**, **g** and **h**), VEGF (**e**) and Shh+VEGF (**f**) induce vessels with different morphology. Red arrowheads indicate the main limbus artery, blue arrowheads indicate the main limbus vein, white arrowheads indicate expanded venous structures and the yellow arrowhead indicates an arteriovenous shunt. **h** shows branching vessels induced by Shh. **i–k**, 5- $\mu$ m cross sections of corneas treated with Shh (**i**), VEGF (**j**) or Shh+VEGF (**k**), immunostained for CD-31 (brown) show differences in vessel diameters induced by each treatment. **l**, Vessel length, circumferential extent of neovascularity and average lumen diameter are significantly higher in Shh-treated corneas. When added to VEGF, Shh is able to increase average vascular lumen diameter (upper right); the large s.e.m. in Shh+VEGF-treated corneas reflects the presence of capillaries and large-diameter vessels. The number of vascular lumens per cross section is higher in VEGF-treated group. \*\*,  $P < 0.0001$ ; \*,  $P < 0.001$ .



chemic hind-limb model, Shh-induced neovascularity consisted of large, branching vessels that grew directly from the limbus vessels and often extended to and surrounded the pellet at the apex of the new vessel growth (Fig. 3b, d, g, h and i). Many of these vessels exhibited dichotomous branching, creating a complex and well-organized vascular tree (Fig. 3h). The average number of branching vessels in corneal neovascularization induced by Shh

was  $7.3 \pm 1.4$  per field (data not shown). In contrast, VEGF implantation resulted in capillaries of lesser luminal caliber that were uniformly distributed along the cornea (Fig. 3a, e and j). Shh-induced neovascularity also exhibited numerous large-diameter vessels that did not arise as branches of the limbus artery, but appeared to be venous structures that often formed arteriovenous shunts (Fig. 3d and g). The average length of Shh-induced neovessels was significantly greater than that of vessels induced by VEGF ( $1.05 \pm 0.18$  versus  $0.67 \pm 0.09$  mm;  $P < 0.0001$ ) (Fig. 3l). The circumferential extent of Shh-induced neovascularity was also increased compared with VEGF ( $190 \pm 3.9$  versus  $116 \pm 9.6$  degrees;  $P < 0.0001$ ) (Fig. 3l). Histological evaluation demonstrated increased luminal diameters in Shh-induced versus VEGF-induced neovessels ( $32.62 \pm 5.82$  versus  $7.25 \pm 0.7$   $\mu$ m;  $P < 0.0001$ ) (Fig. 3i, j and l). In both the Shh and VEGF groups, the number of periendothelial cells was limited with no significant difference ( $3.52 \pm 1.66$  versus  $4.88 \pm 1.75$  smooth muscle cells per cross section, respectively;  $P = \text{NS}$ ) (data not shown). In addition, the combination of Shh and VEGF showed lengthened, large-diameter neovessels like those seen with Shh alone, but also exhibited characteristics of VEGF-induced vasculature, that is, a dense area of fine vessels close to the implanted pellet (Fig. 3f and k). Thus, Shh and VEGF together appeared to produce an intermediate phenotype containing a variety of neovascular lengths and diameters (Fig. 3f, k and l).

#### Ptc1 mediates Shh-induced angiogenesis in fibroblasts

To determine the identity of cells directly activated by Shh during corneal angiogenesis, we implanted pellets containing Shh

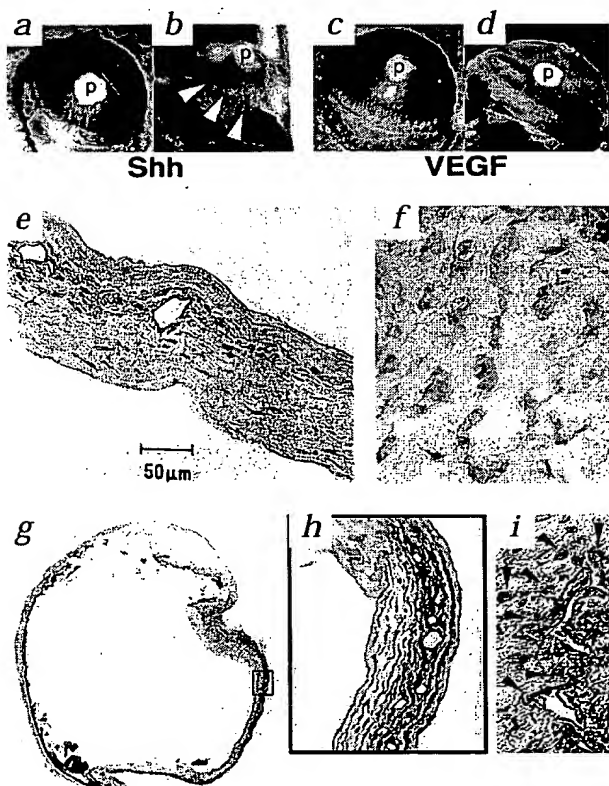


**Fig. 4** Shh acts upon stromal cells and induces VEGF production. **a–d**, Macroscopic photographs of corneal neovascularization induced by pellets ('p') containing Shh (**a**) and VEGF (**c**) and correspondent  $\beta$ -gal staining for Ptc1 in Shh-treated (**b**) and VEGF-treated (**d**) corneas.  $\beta$ -gal-positive staining is detectable in correspondence of Shh-induced angiogenesis (arrowheads in **b**), but not of VEGF-induced angiogenesis (**d**). **e–i**, Cross sections of Shh-treated corneas, prepared as in **b**, immunostained for CD-31 (**e**), vimentin (**f**) or VEGF at magnifications of  $\times 20$  (**g**),  $\times 100$  (**h**) and  $\times 400$  (**i**). VEGF staining is localized only in the neovascular area (**g**), around the neovessels (**h** and **i**). Cells with  $\beta$ -gal-positive nuclei have VEGF-positive cytoplasm (red arrowheads in **i**).

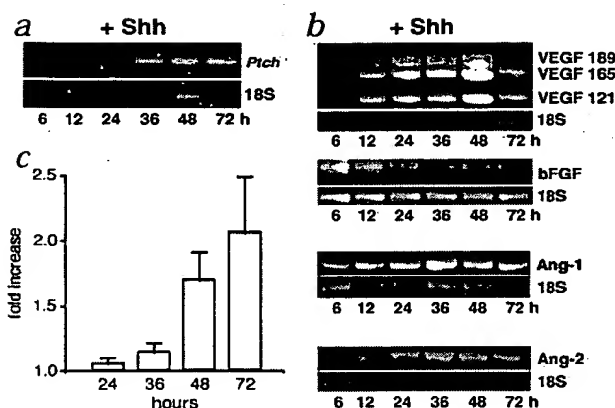


**Fig. 5** Shh upregulates *Ptch*, VEGF and angiopoietins in human fibroblasts. **a** and **b**, Quantitative RT-PCR for *Ptch* (**a**) and angiogenic cytokines (**b**) shows that fibroblasts respond to Shh by upregulating *Ptc1*, all 3 isoforms of VEGF-1, Ang-1 and -2, while bFGF is downregulated. **c**, Conditioned media from Shh-stimulated compared with vehicle-stimulated human lung fibroblasts shows a ~2-fold increase in VEGF<sub>165</sub> (mean  $\pm$  s.e.m.) detected by ELISA between 48 and 72 h in this representative experiment.

treatment (Fig. 5b). These results demonstrate that Shh induces a specific subset of angiogenic growth factors including the VEGF-1 isoforms as well as Ang-1 and Ang-2.

#### Discussion

Our results clearly show that Shh has angiogenic activity. Shh induces robust neovascularization in the setting of ischemia and may have important therapeutic utility in the treatment of ischemic disorders. Neovascularization induced by Shh appears to be mediated by stromal cells producing a combination of potent angiogenic factors, including VEGF, Ang-1 and Ang-2. *In vitro*, most fibroblasts cell lines respond to Shh by *Ptch* upregulation (Fig. 5a and data not shown). However, repeated attempts to activate HUVECs, aortic and microvascular endothelial cells by Shh treatment were unsuccessful. These cells show no proliferation, serum-free survival, migration or upregulation of *Ptc1* in response to Shh proteins (data not shown). *Ptc1* was not upregulated on endothelial cells in Shh-treated corneas or in endothelial cells of aortas from Shh-treated mice. Despite this, endothelial cells do express *Ptc1* *in vitro* and *in vivo* and the possibility that Shh affects endothelial cells cannot therefore be completely excluded.

Our data instead indicate that neovascularization induced by Shh might be triggered through Shh/*Ptc1* signaling specifically in mesenchymal cells. Fibroblasts are a well-known source of VEGF during development, tumor growth, hypoxia and inflammation<sup>31-34</sup>. Our data raise the possibility that VEGF production from fibroblasts might be mediated by the Hh pathway. Similar indirect mechanisms of inducing angiogenesis have been demonstrated for PDGF (platelet-derived growth factor) BB and TGF (tumor growth factor)  $\beta 1$ , both of which promote angiogenesis via upregulation of VEGF and basic fibroblast growth factor (bFGF)<sup>35</sup>. Given this precedent, we propose that Shh acts upon interstitial mesenchymal cells (such as fibroblasts in the cornea) to induce an array of angiogenic growth factors, including three isoforms of VEGF-1 as well as Ang-1 and Ang-2. The ability to upregulate these angiogenic cytokines in concert appears thus far unique to Shh. There are no previous reports of Ang-1 expression being regulated by other cytokines, morphogens, growth factors or ischemia.

Here we show that the angiogenic response to Shh is characterized by long, tortuous vessels with large diameters. It has been shown that vessels with increased length, diameter and branching are induced when Ang-1 acts synergistically with VEGF (ref. 36). We show here that Shh upregulates both VEGF and Ang-1; however, Shh induces an even more complex vascular system. When Shh is used, the quantitative and qualitative features of the vessels are more pronounced and they are also associated with vascular tortuosity. The basis for this remains to be elucidated, but it is possible that exogenous administration of VEGF and Ang-1 together might not be comparable to localized activation of these growth factors in stromal cells by Shh. Localized overexpression of VEGF and Ang-1 in the skin of transgenic mice, for example, produces

or VEGF into the cornea of NLS-*Ptch-lacZ* mice. After collecting them, we stained corneas for  $\beta$ -gal to detect *Ptc1* expression. Strong  $\beta$ -gal staining was detected around the neovascular foci of NLS-*Ptch-lacZ* eyes treated with Shh, indicating that Shh activates the Hh pathway during neovascularization (Fig. 4a and b). In contrast, VEGF-treated corneas were  $\beta$ -gal-negative, indicating that VEGF does not induce expression of *Ptc1* (Fig. 4c and d). Histological analysis showed that  $\beta$ -gal-positive cells were not endothelial cells (CD31-negative) or periendothelial cells ( $\alpha$ -smooth-muscle-actin-negative, data not shown), but were consistent with interstitial fibroblasts (vimentin-positive) surrounding the neovessels (Fig. 4e and f). The  $\beta$ -gal-positive cells as well as their surrounding matrix were also immunopositive for VEGF, indicating that Shh might stimulate—either directly or indirectly—VEGF expression within the neovascular foci (Fig. 4g, h and i).

#### Shh upregulates *Ptch* and induces VEGF and Ang-1 and -2

We tested the possibility that Shh might induce fibroblasts to produce angiogenic cytokines by treating fibroblasts in culture with Shh protein and evaluating the induction of *Ptch*, VEGF and other angiogenic cytokines. Quantitative reverse transcriptase (RT)-PCR showed that a number of primary fibroblasts and fibroblast cell lines responded to Shh stimulation by upregulating *Ptch* (Fig. 5a and data not shown). Comparison of *Ptch* expression in Shh-treated and vehicle-treated fibroblasts at various time points showed that *Ptch* was induced within 6–12 hours after addition of Shh to the medium, and continued to increase up to 72 hours. In contrast, the absence of *Ptch* upregulation by endothelial cells in the corneal neovessels was mirrored *in vitro* by the inability of human umbilical vein endothelial cells (HUVECs) or microvascular endothelial cells to respond to Shh by *Ptch* upregulation, proliferation, migration or serum-free survival (data not shown).

In addition to upregulating *Ptch*, Shh stimulated cultured fibroblasts to increase expression of angiogenic growth factors, including all three isoforms of VEGF-1 and both Ang-1 and Ang-2 (Fig. 5b). Upregulation of mRNA encoding VEGF<sub>121</sub>, VEGF<sub>165</sub> and VEGF<sub>183</sub> was first detected at 12 hours and continued to increase up to 48 hours in Shh-stimulated compared with vehicle-stimulated cells at each time point. This increase in VEGF-1 mRNA correlated with a significant increase in VEGF<sub>165</sub> protein (Fig. 5c). Finally, Shh treatment also upregulated Ang-1 and Ang-2 mRNA (Fig. 5b). In contrast, expression of bFGF was decreased after Shh



similar large-diameter, long and distinctly branching vessels<sup>37</sup>. Moreover, the sequence and magnitude of upregulation of these cytokines by Shh *in vivo* is unknown. Shh also upregulates Ang-2 and all three isoforms of VEGF-1. In colon cancer, compared with tumors expressing only one or two VEGF-1 isoforms, the coordinated expression of three VEGF-1 isoforms correlates with more aggressive tumors, as shown by vein invasion and metastasis leading to a poor prognosis<sup>38</sup>. The particular combination of angiogenic growth factors induced by Shh might thus contribute to the robust and distinct character of its neovascularization.

VEGF has been implicated in the earliest stage of vasculogenesis, during endothelial-cell differentiation and plexus formation, but also in postnatal angiogenesis through its ability to induce endothelial-cell migration and proliferation<sup>39</sup>. Ang-1 is required for both embryonic remodeling of the vascular plexus and postnatal vessel remodeling involving sprouting, branching or vessel maturation<sup>39</sup>. *In vivo* studies reveal that Ang-1 acts in a complementary and coordinated fashion with VEGF, mediating interactions between endothelial cells and surrounding support cells<sup>40</sup>. Ang-2 acts as a natural antagonist of Ang-1 (ref. 40). Whereas Ang-1 is expressed widely in normal adult tissues, Ang-2, in its role in continuous vascular stabilization, is highly expressed only at sites of vascular remodeling in order to allow the vessels to revert to a more plastic and unstable state<sup>40</sup>. Ang-2 is expressed along with VEGF in tumor vasculature and the two together might function as an angiogenic signal at the growing periphery of tumors<sup>40</sup>. Our study indicates that Shh upregulates both Ang-1 and Ang-2. The significance and relevance of this concomitant activation is unclear. We suggest that in the case of Shh-induced angiogenesis, VEGF might initiate the angiogenic response and angiopoietins could subsequently antagonize each other in a complex process of recruitment, stabilization and remodeling of neovascularization.

Shh-induced vessels tend to bifurcate into two branches that eventually split again. Previous reports show that tracheal splitting and branching during lung organogenesis are regulated by the Hh/Ptc1/Gli pathway through a number of effects including FGF inhibition<sup>3</sup>. We observed evidence of bFGF downregulation in fibroblasts treated with Shh, and that the Shh-induced vessels are highly branched. The vascular network induced by Shh is also characterized by several venous structures with arteriovenous shunts. This vasculature is functional, as demonstrated by the increase in perfusion and consequent rate of limb salvage in aged mice with limb ischemia. These experiments indicate that Shh might have therapeutic uses in promoting angiogenesis in the ischemic disorders.

The signaling pathway by which Hh upregulates these angiogenic growth factors remains to be determined. *Ptc1* and many other Hh-inducible genes are regulated by the Hh pathway transcriptional factor Gli. However, no Gli response elements are present in the VEGF or Ang-1 promoter regions. Hh can, however, also induce a Gli-independent pathway that activates the orphan nuclear receptor, COUPTFII (ref. 41). Interestingly, COUPTFII-deficient embryos are defective in maturation of the primary vascular plexus and exhibit decreased Ang-1 expression<sup>42</sup>. Thus it is possible that Hh induces at least Ang-1 via COUPTFII activation in mesenchymal cells.

The development of functional vasculature requires precise spatial-temporal regulation of cell proliferation, migration, interaction and differentiation. The role of Shh as a morphogen might be relevant to its potential activity to orchestrate appro-

prate spatial-temporal production of angiogenic growth factors during embryonic and postnatal angiogenesis, which in addition must be coordinated with muscle, bone and nerve development. This report thus establishes novel biological and potentially therapeutic activities for Shh. The discovery of angiogenic activity for Shh, combined with its known morphogenic functions in development, indicates that Shh might coordinate epithelial/stromal interactions with the ingrowth of vasculature during development. Given that Shh can promote limb salvage in aged mice through the enhancement of blood flow and capillary density and induction of large caliber vessel formation, we suggest that Shh merits investigation as proangiogenic therapy for ischemic disorders.

## Methods

**Mice.** Male C57BL/6J mice (Jackson Labs, Bar Harbor, Maine), heterozygous male or female *NLS-Ptc1-lacZ* mice or their wild-type littermates (Ontogeny, Cambridge, Massachusetts) were used. All experiments were conducted in accordance with St. Elizabeth's or Biogen Institutional Animal Care and Use Committee.

**Systemic treatment with Shh.** Postnatal day 6 *NLS-Ptc1-lacZ* mice were treated with daily subcutaneous injections of 10–20  $\mu$ L of polyethylene glycol 20,000-conjugated C24II/A192C Shh N-terminal protein or vehicle<sup>43</sup>. Hearts and aortas were collected at postnatal day 9 and stained for  $\beta$ -gal expression.

**Ischemic hind-limb model.** Unilateral hind-limb ischemia was created in 2-year-old C57BL/6J mice<sup>44</sup>. Eighty mice were operated and treated with intramuscular injections of 1 mg/kg Shh–mIgG1 fusion protein, vehicle or 100  $\mu$ g/kg of rhVEGF<sub>165</sub> (Chemicon, Temecula, California). Injections were once every other day during the first week, once every 3 days during the second week, and twice during the third and fourth weeks. At predetermined time points, necrosis and hind-limb perfusion were examined by two blinded operators<sup>44</sup>. Mice were then killed for histological analysis. Hind limbs were fixed in 100% methanol and cut in paraffin sections. Capillaries were counted by two blinded observers<sup>44</sup>. Shh–mIgG1 has increased half-life and activity *in vivo* (Shapiro *et al.*, manuscript in preparation). It contains residues Cys24–Gly197 of the human Shh coding sequence with two mutations: Cys24Ilelle and KRRH(32–35)QRRP, with a 16-fold increased activity *in vitro* compared with unmodified mature human Shh protein produced *E. coli* (Taylor *et al.*, manuscript in preparation). The Fc region of mouse IgG1 was fused directly downstream of Gly127. The glycosylation site was destroyed with a Gln to Asn mutation. Protein was expressed in *Pichia pastoris* GS115 (Invitrogen, Carlsbad, California) using a pPIC9-derived vector and the  $\alpha$ -mating-factor secretion signal. The protein was purified and sequenced as described<sup>10,45</sup>.

**Cornea neovascularization assay.** Pellets containing one of the following were implanted in C57BL/6J mice<sup>46</sup>: 1.5  $\mu$ g myristoylated-Shh protein (Myr-Shh), 0.3  $\mu$ g VEGF (R&D Systems, Minneapolis, Minnesota), 1.5  $\mu$ g Myr-Shh + 0.3  $\mu$ g VEGF, or vehicle. In *NLS-Ptc1-lacZ* mice pellets contained Myr-Shh 1.5  $\mu$ g/pellet, VEGF 0.3  $\mu$ g/pellet or vehicle. Myr-Shh was prepared by chemical myristoylation (Taylor *et al.*, manuscript in preparation) of the  $\alpha$ -amino group of Cys24 (of *E. coli*-produced mature human Shh protein) followed by repurification and sequencing<sup>10,45</sup>. Myr-Shh exhibited 160-fold increased activity *in vitro* compared with mature human Shh protein (Cys24–Gly197).

**Histology.** Tissues from *NLS-Ptc1-lacZ* mice were fixed in 0.2% glutaraldehyde, washed, stained overnight at 37 °C in 1 mg/mL X-gal, 5 mM potassium ferricyanide, 5 mM potassium ferrocyanide, 2 mM MgCl<sub>2</sub>, 0.01% sodium deoxycholate, 0.02% Nonidet P-40, 50 mM Na<sub>2</sub>HPO<sub>4</sub>, pH8, and visualized as whole mounts or paraffin sections. For immunohistochemistry, eyes were fixed in 100% methanol or in 1% paraformaldehyde. Corneal hemispheres were cut into paraffin or frozen sections. Endothelial cells were identified using rat monoclonal antibody against mouse CD31 (Pharmingen, San Diego, California) and a biotinylated goat



immunoglobulin against rat. For periendothelial cells, a mouse monoclonal antibody against smooth muscle  $\alpha$ -actin conjugated with alkaline phosphatase (Sigma) was used. For VEGF, a rabbit polyclonal antibody against VEGF (Santa Cruz Biotechnology, Santa Cruz, California) and a biotinylated goat immunoglobulin antibody against rabbit (Signet Labs, Dedham, Massachusetts) were used. Staining for vimentin was done with goat serum against vimentin (Sigma) compared with normal goat serum (Sigma) using horseradish peroxidase-conjugated donkey secondary antibody against goat (Jackson Immunoresearch, West Grove, Pennsylvania). For fluorescence microscopy, mice received an intravenous bolus of 500  $\mu$ g of FITC-conjugated BS-1 lectin (Vector, Burlingame, California) 30 min before death. Eyes were fixed in 1% paraformaldehyde, and the dissected corneas were placed on glass slides.

**Competitive RT-PCR.** RNA was extracted from CCD37 human lung fibroblasts (ATCC) stimulated *in vitro* with MyrShh or vehicle. cDNA was obtained and amplified using the SuperScript preamplification system (Gibco-BRL, Paisley, UK). Signals were normalized to 18S rRNA using optimal 18S primer/Competimer ratios as determined for each target gene following the manufacturer's recommendations (Ambion, Austin, Texas) or to GAPDH, using GAPDH control reagents and Taqman analysis (PE Applied Biosystems, Foster City, California). The following primer pairs and PCR conditions were used. Ptc1: 5'-TCAGGATGCATTTGACAGT-GACTGG-3' and 5'-ACTCCGAGTCGGAGGAATCAGACCC-3' with 25 cycles of 94 °C (30 s), 55 °C (1 min) and 72 °C (1 min). VEGF: 5'-CGAAGTGGTGAAGTTCATGGATG-3' and 5'-TTCTGTATCAGCTTTCTGGTGAG-3' with 30 cycles of 94 °C (30 s), 62 °C (1 min) and 72 °C (1 min). bFGF: 5'-TACAATTCACAGCAGAAGAG-3' and 5'-CAGCTCTTAGCAGACATTGG-3' with 25 cycles of 94 °C (30 s), 62 °C (1 min), and 72 °C (1 min). Ang-1: 5'-CAACACAACGCTCTGCAGAGAGA-3' and 5'-CTCCAGTTGCTGCTTCTGAAGGAC-3' with 25 cycles of 94 °C (30 s) and 64 °C (90 s). Ang-2: 5'-AGCGACGTGAGGATGGCAGCGTT-3' and 5'-ATTCTCTGGTTGGCTGATGCTGCTT-3' with 32 cycles of 94 °C (30 s) and 64 °C (90 s).

**ELISA.** VEGF<sub>165</sub> in conditioned media from MyrShh-stimulated cells were compared with vehicle-stimulated cells. VEGF<sub>165</sub> was measured per manufacturer's instructions using the Quantikine human VEGF-ELISA kit (R&D Systems, Minneapolis, Minnesota). All experiments were performed in triplicate.

**Statistical analysis.** All results are expressed as mean  $\pm$  s.e.m. Differences were analyzed by ANOVA or  $\chi$ -square test and considered statistically significant at  $P < 0.05$ .

#### Acknowledgments

We thank K. Strauch and E. Garber for the design and generation of recombinant Shh-mIgG1 fusion protein and J. Mead, E. Barban and T. Aprahamian for technical assistance.

RECEIVED 24 JANUARY; ACCEPTED 30 APRIL 2001

- Chiang, C. *et al.* Cyclopia and defective axial patterning in mice lacking sonic hedgehog gene function. *Nature* **383**, 407–413 (1996).
- Johnson, R.L. & Tabin, C.J. Molecular models for vertebrate limb development. *Cell* **90**, 979–990 (1997).
- Pepicelli, C.V., Lewis, P.M. & McMahon, A.P. Sonic hedgehog regulates branching morphogenesis in the mammalian lung. *Curr. Biol.* **8**, 1083–1086 (1998).
- Ramalho-Santos, M., Melton, D.A. & McMahon, A.P. Hedgehog signals regulate multiple aspects of gastrointestinal development. *Development* **127**, 2763–2772 (2000).
- St-Jacques, B. *et al.* Sonic hedgehog signaling is essential for hair development. *Curr. Biol.* **8**, 1058–1068 (1998).
- St-Jacques, B., Hammerschmidt, M. & McMahon, A.P. Indian hedgehog signaling regulates proliferation and differentiation of chondrocytes and is essential for bone formation. *Genes Dev.* **13**, 2072–2086 (1999).
- Bitgood, M.J., Shen, L. & McMahon, A.P. Sertoli cell signaling by Desert hedgehog regulates the male germline. *Curr. Biol.* **6**, 298–304 (1996).
- Parmantier, E. *et al.* Schwann cell-derived Desert hedgehog controls the development of peripheral nerve sheaths. *Neuron* **23**, 713–724 (1999).
- Porter, J.A., Young, K.E. & Beachy, P.A. Cholesterol modification of hedgehog signaling proteins in animal development. *Science* **274**, 255–259 (1996).
- Pepinsky, R.B. *et al.* Identification of a palmitic acid-modified form of human Sonic hedgehog. *J. Biol. Chem.* **273**, 14037–14045 (1998).
- Fuse, N. *et al.* Sonic hedgehog signals not as a hydrolytic enzyme but as an apparent ligand for patched. *Proc. Natl. Acad. Sci. USA* **96**, 10992–10999 (1999).
- Zardoya, R., Abouheif, E. & Meyer, A. Evolution and orthology of hedgehog genes. *Trends Genet.* **12**, 496–497 (1996).
- Bitgood, M.J. & McMahon, A.P. Hedgehog and Bmp genes are coexpressed at many diverse sites of cell-cell interaction in the mouse embryo. *Dev. Biol.* **172**, 126–138 (1995).
- Ingham, P.W. Transducing hedgehog: the story so far. *EMBO J.* **17**, 3505–3511 (1998).
- Stone, D.M. *et al.* Characterization of the human suppressor of fused, a negative regulator of the zinc-finger transcription factor Gli. *J. Cell. Sci.* **112**, 4437–4448 (1999).
- Kogerman, P. *et al.* Mammalian Suppressor-of-Fused modulates nuclear-cytoplasmic shuttling of Gli-1. *Nature Cell. Biol.* **1**, 312–319 (1999).
- Ding, Q. *et al.* Mouse suppressor of fused is a negative regulator of sonic hedgehog signalling and alters the subcellular distribution of Gli. *Curr. Biol.* **9**, 1119–1122 (1999).
- Monnier, V., Dussillol, F., Alves, G., Lamour-Isnard, C. & Plessis, A. Suppressor of fused links fused and Cubitus interruptus on the hedgehog signaling pathway. *Curr. Biol.* **8**, 583–586 (1998).
- Sisson, J.C., Ho, K.S., Suyama, K. & Scott, M.P. Costal2, a novel kinesin-related protein in the Hedgehog signaling pathway. *Cell* **90**, 235–245 (1997).
- Robbins, D.J. *et al.* Hedgehog elicits signal transduction by means of a large complex containing the kinesin-related protein costal2. *Cell* **90**, 225–234 (1997).
- Kalderon, D. Hedgehog signalling: Cl complex cuts and clasps. *Curr. Biol.* **7**, R759–R762 (1997).
- Marigo, V., Johnson, R.L., Vortkamp, A. & Tabin, C. Sonic hedgehog differentially regulates expression of Gli1 and Gli3 during limb development. *Dev. Biol.* **180**, 273–283 (1996).
- Marigo, V. & Tabin, C. Regulation of patched by sonic hedgehog in the developing neural tube. *Proc. Natl. Acad. Sci. USA* **93**, 9346–9351 (1996).
- Rowitch, D.H. *et al.* Sonic hedgehog regulates proliferation and inhibits differentiation of CNS precursor cells. *J. Neurosci.* **19**, 8954–8965 (1999).
- Brown, L.A. *et al.* Insights into early vasculogenesis revealed by expression of the ETS-domain transcription factor Fli-1 in type and mutant zebrafish embryos. *Mech. Dev.* **90**, 237–252 (2000).
- Vu, T.H. *et al.* MMP-9/gelatinase B is a key regulator of growth plate angiogenesis and apoptosis of hypertrophic chondrocytes. *Cell* **93**, 411–422 (1998).
- Zhou, Z. *et al.* Impaired endochondral ossification and angiogenesis in mice deficient in membrane-type matrix metalloproteinase 1. *Proc. Natl. Acad. Sci. USA* **97**, 4052–4057 (2000).
- Mecklenburg, L. *et al.* Active hair growth (anagen) is associated with angiogenesis. *J. Invest. Dermatol.* **114**, 909–916 (2000).
- Wang, L.C. *et al.* Conditional disruption of hedgehog signaling pathway defines its critical role in hair development and regeneration. *J. Invest. Dermatol.* **114**, 901–908 (2000).
- Rivard, A. *et al.* Age-dependent impairment of angiogenesis. *Circulation* **99**, 111–120 (1999).
- Scheid, A. *et al.* Hypoxia-regulated gene expression in fetal wound regeneration and adult wound repair. *Pediatr. Surg. Int.* **16**, 232–236 (2000).
- Volpert, O.V., Dameron, K.M. & Bouck, N. Sequential development of an angiogenic phenotype by human fibroblasts progressing to tumorigenicity. *Oncogene* **14**, 1492–1502 (1997).
- Detmar, M. *et al.* Hypoxia regulates the expression of vascular permeability factor/vascular endothelial growth factor (VPF/VEGF) and its receptor in human skin. *J. Invest. Dermatol.* **108**, 263–268 (1997).
- Cho, C.S. *et al.* CD40 engagement on synovial fibroblasts up-regulates production of vascular endothelial growth factor. *J. Immunol.* **164**, 5055–5061 (2000).
- Brögl, E. *et al.* Indirect angiogenesis cytokines upregulate VEGF and bFGF gene expression in vascular smooth muscle cells, while hypoxia upregulates VEGF expression only. *Circulation* **90**, 649–652 (1994).
- Asahara, T. *et al.* Tie2 receptor ligands, angiopoietin-1 and angiopoietin-2, modulate VEGF-induced postnatal neovascularization. *Circ. Res.* **83**, 233–240 (1998).
- Suri, C. *et al.* Increased vascularization in mice overexpressing angiopoietin-1. *Science* **282**, 468–471 (1998).
- Tokunaga, T. *et al.* Vascular endothelial growth factor (VEGF) mRNA isoforms expression pattern is correlated with liver metastasis and poor prognosis in colon cancer. *Br. J. Cancer* **77**, 998–1002 (1998).
- Gale, N.W. & Yancopoulos, G.D. Growth factors acting via endothelial cell-specific receptor tyrosine kinases: VEGFs, angiopoietins, and ephrins in vascular development. *Genes Dev.* **13**, 1055–1066 (1999).
- Holash, J. *et al.* New model of tumor angiogenesis: dynamic balance between vessel regression and growth mediated by angiopoietins and VEGF. *Oncogene* **18**, 5356–5362 (1999).
- Krishnan, V. *et al.* Mediation of Sonic hedgehog-induced expression of COUP-TFII by a protein phosphatase. *Science* **278**, 1947–1950 (1997).
- Pereira, F.A. *et al.* The orphan nuclear receptor COUP-TFII is required for angiogenesis and heart development. *Genes Dev.* **13**, 1037–1049 (1999).
- Pepinsky, R.B. *et al.* Mapping sonic hedgehog-receptor interactions by steric interference. *J. Biol. Chem.* **275**, 10995–11001 (2000).
- Couffignal, T. *et al.* A mouse model of angiogenesis. *Am. J. Pathol.* **152**, 1667–1679 (1998).
- Williams, K.P. *et al.* Functional antagonists of sonic hedgehog reveal the importance of the N terminus for activity. *J. Cell. Sci.* **112**, 4405–4414 (1999).